IMPERIAL COLLEGE LONDON

DEPARTMENT OF MATHEMATICS

SECOND-YEAR GROUP RESEARCH PROJECT

Stochastic Resetting and its Applications

Authors:
Vasudev Joy (CID: 02016170)
Ben Le Jeune (CID: 02232503)
James Corcoran (CID: 02220389)
Pip Moss (CID: 02226404)
Charalampos Zacharia (CID: 02033690)

Supervisor:
Dr Thibault Bertrand

June 17, 2024

Abstract

In this review paper, we present key results about stochastic resetting in one and two dimensions for two different models for motion. We begin with the simple case of a purely diffusive particle under Poissonian resetting to a fixed position with constant rate and consider some key results, such as the existence of a non-equilibrium steady state (which is trivial without resetting). A key idea throughout this review is the use of stochastic resetting in optimising search algorithms, by minimising the mean first-passage time. We study this under different resetting mechanisms, such as time- and space-dependent resetting. We then consider a second model of motion which is of critical importance in biological applications: the run-and-tumble model. We explore the impact of resetting on run-and-tumble particles, and find non-equilibrium steady states. Finally, we consider the use of resetting in various target-search problems (e.g absorption to a spherical target at the origin or the presence of multiple static traps) and compare simulated results for run-and-tumble motion with those for diffusion.

Contents

1 Introduction

What you are looking for could be right under your nose - you just missed it. This is why often, after failing to find a lost item, we return to the starting point of our search and try again. This is an example of a search process, and these are pervasive in science and nature. They arise when animals forage for food [1, 2], in chemical reactions [3], and even evolution [2].

This intuitive need to optimise searching has a mathematical basis. If we use Brownian motion as a model for our searching, a well-known result is that the expected time to reach your target is infinite in one [4] and two [5] dimensions. Many of the search processes above, such as animal foraging, follow an *intermittent search strategy* [1, 6]: random periods of searching interspersed with long moves. These have been shown to increase efficiency in the long-term [7].

1.1 Stochastic resetting

Another strategy is to return to your starting point rather than using a purely diffusive or intermittent search strategy. When you return to the starting point at random times, this process is called *stochastic resetting*. This has been an area of interest in recent years, particularly when applied to diffusion, as there are several significant changes to the dynamics of the system [4]. In particular, the average time taken to reach a target for the first instance - *mean first-passage time*, or MFPT - becomes finite, since there is an effective limit on how 'lost' a searching particle can become. Furthermore, the system admits a steady-state distribution [8]. This steady state is non-equilibrium, since there are probability currents that correspond to particles resetting. These properties and others are summarised in a review by Evans et al. [4]. However, modelling resetting as instantaneous is divorced from the reality of experiments, in which resetting occurs over a nonzero time frame. More detailed cases explored recently include the imposition of a refractory period before the search continues after resetting [9] and resetting to the initial position with a fixed velocity [9], where a low resetting rate can improve the MFPT, whereby conditions are imposed upon the coefficient of variation. Other objects of study include the effects of resetting in the presence of multiple targets [9] in various arrangements [10], leading to unexpected conclusions. For example, increasing the distance between targets can decrease the overall search time [10].

We can also begin to optimise resetting rates in order to minimise the MFPT. It can be shown that there exists an optimal resetting rate such that the MFPT attains a minimum under Poissonian resetting. Non-Poissonian resetting rates have also been considered, including various time- [11] and space- [12] dependent rates , including deterministic resetting intervals. It remains an open question whether there exists a globally minimising space-dependent rate function.

1.2 Asymptotic behaviours

Resetting can also affect asymptotic behaviours of diffusive systems. A diffusive particle (or a density of particles) in a sea of traps has been studied in a chemical context [13] for various types of reaction. It is well-known that in such systems with static traps [14], particle density decays slower than exponentially. The bases for these claims are rendered invalid under stochastic resetting to a random position, which is analogous to restarting the process. Further areas of study include systems of diffusing traps [15], such as coordinating traps [16].

1.3 Run-and-tumble motion

As well as considering the addition of resetting to a purely diffusive process, we may also consider its impact on the movement of bacteria. Bacteria move according to 'run-and-tumble' motion, consisting of movement in a straight line ('runs'), which are broken up by random changes in orientation ('tumbles') [17]. It is known that *at large time-scales*, this motion is diffusive in the so-called *diffusive limit* [18]. However, on short time-scales, run-and-tumble motion is ballistic, and therefore we expect to observe different behaviour.

1.4 This paper

In this review, we establish many known results about stochastic resetting in one- and two-dimensional diffusion in various environments, including deriving the non-equilibrium steady states, the mean first-passage times (MFPT) and survival probabilities. We contrast this behaviour with that of a run-and-tumble particle under resetting, recovering the original results in the diffusive limit. We also establish analytically (in one dimension) and numerically (in two dimensions) the differences in behaviour between diffusive and run-and-tumble particles, particularly at short time-scales. Furthermore, we show numerically that stochastic resetting can recover the expected decay behaviour of a diffusive particle in a uniform density of traps, and compare this with a diffusion process in a sea of deterministic traps.

2 Stochastic resetting for a diffusive particle in 1D

In this section, we consider the diffusion of a single particle along the real line and introduce resetting to this model. Importantly, we observe that the introduction of resetting now admits a non-equilibrium steady state. We start with the addition of Poissonian resetting to a purely diffusive particle, before extending this to a drift-diffusion process and consider the effect of resetting to a probability distribution. We conclude this section with an assessment of how different methods of resetting, such as time- and space-dependent resetting, improve a purely diffusive model in a target-search problem.

2.1 The Fokker-Planck equation and its steady-state limit

In order to analyse one-dimensional diffusion under Poissonian resetting, we consider a single particle on the real line with initial position x_0 and which resets to a position or distribution X_r at rate r. For $p(x,t)$, the probability of the particle being in position x at time t, the Fokker-Planck equation[1] for this model is known [4], and is given by

$$\frac{\partial p(x,t|x_0)}{\partial t} = D\frac{\partial^2 p(x,t|x_0)}{\partial x^2} - rp(x,t|x_0) + r\delta(x - X_r), \tag{1a}$$

$$p(x,0|x_0) = \delta(x - x_0). \tag{1b}$$

Equation (1a) is a well-known result, so we do not derive it. Instead, we present an interpretation of each term, to illuminate further the key aspects of this model.

For this initial model, we add stochastic resetting to a particle undergoing purely diffusive motion. One can see this in equation (1a) with $r = 0$. Therefore, the terms $\frac{\partial p(x,t|x_0)}{\partial t} =$

[1] A Fokker-Planck equation is a PDE which defines the time evolution of a probability density function. Fokker-Planck equations are also commonly referred to as forward Kolmogorov equations. We will encounter backward Kolmogorov/master equations in subsequent sections.

$D\frac{\partial^2 p(x,t|x_0)}{\partial x^2}$ represent the underlying diffusion in this system. The resetting terms, $-rp(x,t)$ and $r\delta(x-X_r)$, can be understood as follows: when a reset occurs (which is governed by the rate, r), the particle is removed from position x at time t, where it exists with probability $p(x,t|x_0)$. Therefore, this removal is represented by the $-rp(x,t|x_0)$ term. This particle is not removed from the entire system; it is instead set to $x = X_r$. Therefore, at each reset there is an addition to $x = X_r$ only. This justifies the $r\delta(x-X_r)$ term.

We begin our analysis of this system by considering its non-equilibrium steady state, which is attained as $t \to \infty$. This is fundamentally different from the long-time behaviour of a diffusive process without resetting, since, as $t \to \infty$, we would instead observe a trivial steady-state solution. We denote the steady-state solution by $p_\infty(x|x_0)$[2], which is no longer time-dependent. In the steady-state limit, we have $\frac{\partial p_\infty(x|x_0)}{\partial t} = 0$. Thus, the steady-state PDF solves the equation

$$D\frac{\partial^2 p_\infty(x|0)}{\partial x^2} - rp_\infty(x|0) + r\delta(x) = 0, \tag{2}$$

where we have let $x_0 = X_r = 0$ for convenience. For the sake of simplicity, we will write $p_\infty(x) \equiv p_\infty(x|x_0)$.

2.1.1 A Fourier method to solve the steady-state problem

The master equation can be solved by a variety of means. We first present a solution using a Fourier transform. Letting $\tilde{p}(k) \equiv \mathcal{F}\{p_\infty(x)\} = \int_{-\infty}^{\infty} p_\infty(x)e^{-ikx}dx$, taking a Fourier transform of equation (2) gives that $-Dk^2\tilde{p}(k) - r\tilde{p}(k) + r = 0$. Rearranging, we obtain an explicit expression for the Fourier transform $\tilde{p}(k)$,

$$\tilde{p}(k) = \frac{r}{Dk^2 + r}. \tag{3}$$

Therefore, by taking the inverse of equation (3), we obtain an explicit integral expression for $p_\infty(x)$.

$$p_\infty(x) = \mathcal{F}^{-1}\{\tilde{p}(k)\} = \frac{1}{2\pi}\int_{-\infty}^{\infty} \frac{r}{Dk^2 + r}e^{ikx}dk. \tag{4}$$

In order to solve this, we shall employ Cauchy's residue theorem with the two cases $x > 0$ and $x < 0$. We also define the key quantity $\alpha_0 \equiv \sqrt{r/D}$.

Case 1: $x > 0$. We consider the semi-circular contour $\Gamma = \Gamma_1 \cup \Gamma_2$, where $\Gamma_1 = \{z = k + 0i : k \in (-R, R)\}$ and $\Gamma_2 = \{z = Re^{i\theta} : \theta \in [0, \pi]\}$, for some $R > \alpha_0$. Now, we consider the integral

$$\oint_\Gamma \alpha_0^2 \frac{e^{izx}}{z^2 + \alpha_0^2}dz. \tag{5}$$

In order to use Cauchy's residue theorem, we consider the poles of $f(z) = \alpha_0^2\frac{e^{izx}}{z^2+\alpha_0}$. Clearly, $f(z)$ has two poles, at $z = \pm i\alpha_0$. Both poles have order 1, and only $z = i\alpha_0$ is internal to Γ. Hence, the value of expression (5) is $2\pi i$ Res$[f(z), i\alpha_0] = \pi\alpha_0\text{exp}(-\alpha_0 x)$. Splitting the contour integral into its two constituent path integrals, we observe that

$$\pi\alpha_0\text{exp}(-\alpha_0 x) = \int_{\Gamma_1} \alpha_0^2 \frac{e^{izx}}{z^2 + \alpha_0^2}dz + \int_{\Gamma_2} \alpha_0^2 \frac{e^{izx}}{z^2 + \alpha_0^2}dz \tag{6}$$

[2]It is common to see the steady-state limit be denoted by $p^*(x|x_0)$. We have elected not to use this notation to clarify that the steady-state limit is not an equilibrium.

Using the natural parametrisations $z = k$ on Γ_1 and $z = Re^{i\theta}$ on Γ_2, we find that equation (6) becomes

$$\pi\alpha_0 \exp(-\alpha_0 x) = \int_{-R}^{R} \alpha_0^2 \frac{e^{ikx}}{k^2+\alpha_0^2} dk + \int_0^{\pi} \alpha_0^2 \frac{e^{iRe^{i\theta}x}}{R^2e^{2i\theta}+\alpha_0^2} Rie^{i\theta} d\theta. \tag{7}$$

Upon consideration of the final term, we observe, by the estimation lemma, that

$$\left| \int_0^{\pi} \alpha_0^2 \frac{e^{iRe^{i\theta}x}}{R^2e^{2i\theta}+\alpha_0^2} Rie^{i\theta} d\theta \right| \leq \pi \max_{\theta\in[0,\pi]} \left| \alpha_0^2 Rie^{i\theta} \frac{e^{iRe^{i\theta}x}}{R^2e^{2i\theta}+\alpha_0^2} \right|.$$

Letting $e^{i\theta} = a + ib$ (where, on Γ_2, $b \leq 0$), we can simplify this upper bound to

$$\alpha_0^2 R \left| \frac{e^{iRe^{i\theta}x}}{R^2e^{2i\theta}+\alpha_0^2} \right| = \alpha_0^2 R \left| \frac{e^{iR(a+ib)x}}{R^2e^{2i\theta}+\alpha_0^2} \right| = \alpha_0^2 R \left| \frac{e^{-Rbx}}{R^2e^{2i\theta}+\alpha_0^2} \right|.$$

As $R \to \infty$, $e^{-Rbx} \to 0$ faster than any power of R. Hence,

$$\left| \int_0^{\pi} \alpha_0^2 \frac{e^{iRe^{i\theta}x}}{R^2e^{2i\theta}+\alpha_0^2} Rie^{i\theta} d\theta \right| \to 0.$$

Therefore, by taking $R \to \infty$,

$$\int_{-\infty}^{\infty} \alpha_0^2 \frac{e^{ikx}}{k^2+\alpha_0^2} dk = \pi\alpha_0 \exp(-\alpha_0 x). \tag{8}$$

Case 2: $x < 0$**.** This case follows in a similar manner. One instead defines Γ_2 as $\{z = Re^{i\theta} : \theta \in [0, -\pi]\}$, where the interval $[0, -\pi]$ denotes that Γ is to be traversed clockwise.

Very similar calculations as in case 1 have been omitted, and we find that for $x < 0$,

$$\int_{-\infty}^{\infty} \alpha_0^2 \frac{e^{ikx}}{k^2+\alpha_0^2} dk = \pi\alpha_0 \exp(\alpha_0 x). \tag{9}$$

Finally, combining equations (8) and (9) gives

$$\int_{-\infty}^{\infty} \alpha_0^2 \frac{e^{ikx}}{k^2+\alpha_0^2} dk = \pi\alpha_0 \exp(-\alpha_0 |x|). \tag{10}$$

This gives an explicit form for the steady-state solution

$$p_\infty(x) = \frac{1}{2}\sqrt{\frac{r}{D}} \exp\left(-\sqrt{\frac{r}{D}}|x| \right). \tag{11}$$

2.1.2 Solving the steady-state problem with Green's functions

Obtaining the steady-state solution by means of a Fourier transform is a valuable tool, but it relies on finding an appropriate contour for the complex integral and gives no insight into a transient solution. Therefore, it is natural to ask whether there exists a more direct method to come to the solution given by equation (11). We will now come to a steady-state solution using Green's functions, which are of critical importance in solving such problems analytically. The

Green's function for the diffusion equation is known [19], and we therefore consider the impact of resetting on this equation, presenting and solving a last renewal equation[3] for this problem.

In the absence of resetting, we have a diffusion problem. Here, $\hat{p}(x,t|x_0)$ is the time-dependent solution to $\frac{\partial \hat{p}}{\partial t} = D\frac{\partial^2 \hat{p}}{\partial x^2}$. By introducing the initial condition $\hat{p}(x,0|x_0) = \delta(x-x_0)$, we recover that $\hat{p}(x,t|x_0) = G_0(x,t|x_0)$, the diffusive Green's function,

$$G_0(x,t|x_0) = \frac{1}{(4\pi D t)^{\frac{1}{2}}} \exp\left(-\frac{|x-x_0|^2}{4Dt}\right) \tag{12}$$

We now add Poissonian resetting with rate r to equation (12). To achieve this, we note that

$$\mathbb{P}(\text{No reset before time = t}) = e^{-rt},$$
$$\mathbb{P}(\text{Last reset at time} = t-\tau) = re^{-r\tau},$$

where the first expression is called the *survival probability for resetting*. Using these, we obtain the last renewal equation for p:

$$p(x,t|x_0) = e^{-rt}G_0(x,t|x_0) + r\int_0^t d\tau e^{-r\tau} G_0(x,\tau|X_r). \tag{13}$$

This is an explicit form of the time-dependent solution to equation (1a). In order to examine properties of the steady state, we take the limit of equation (13) as $t \to \infty$ and set $x_0 = X_r$ for the sake of simplicity. Thus, we obtain

$$p_\infty(x|x_0) = r\int_0^\infty d\tau e^{-r\tau} G_0(x,\tau|X_r). \tag{14}$$

Using the specific G_0 for the case of a purely diffusive particle, as in equation (12), we uncover an integral form for p_∞:

$$p_\infty(x|x_0) = \frac{r}{(4\pi D)^{\frac{1}{2}}}\int_0^\infty d\tau \cdot \tau^{-\frac{1}{2}} \exp\left(-\frac{|x-x_0|^2}{4D\tau} - r\tau\right). \tag{15}$$

Letting $\beta = \frac{|x-x_0|^2}{4D}$ and $\gamma = r$, the right hand side of equation (15) becomes

$$\frac{r}{(4\pi D)^{\frac{1}{2}}}\int_0^\infty d\tau \cdot \tau^{-\frac{1}{2}} \exp\left(-\frac{\beta}{\tau} - \gamma\tau\right).$$

We evaluate this integral using the identity $\int_0^\infty dt \cdot t^{\nu-1}\exp\left(-\beta/t - \gamma t\right) = 2\left(\beta/\gamma\right)^{\nu/2} K_\nu\left(2\sqrt{\beta\gamma}\right)$ given in [20], obtaining

$$p_\infty(x|x_0) = \frac{r}{(4\pi D)^{\frac{1}{2}}} \cdot 2\left(\frac{\beta}{\gamma}\right)^{\frac{1}{4}} K_{1/2}(2\sqrt{\beta\gamma}), \tag{16}$$

where $K_\nu(y)$ denotes the modified Bessel function of the second kind of order ν. For $\nu = 1/2$, we use the known identity $K_{1/2}(y) = \left(\frac{\pi}{2y}\right)^{1/2} e^{-y}$ [20], which gives us the explicit solution

$$p_\infty(x|x_0) = \frac{r}{2D^{\frac{1}{2}}}\gamma^{-\frac{1}{2}} \exp\left(-2\sqrt{\beta\gamma}\right). \tag{17}$$

[3] The last renewal equation conditions on the time of the last reset and considers diffusion since then. There also exists a *first renewal equation*, which will be seen in section 2.3.3.

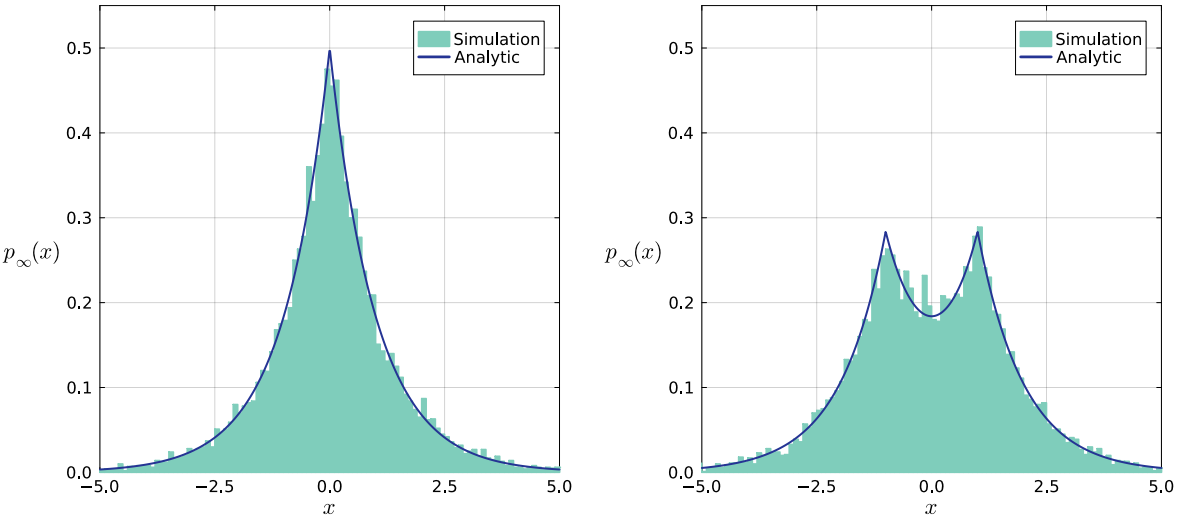

(a) Stochastic resetting to the origin

(b) Stochastic resetting to 1 or -1.

Figure 1 Analytic solution, given in equation (18), is plotted against numerical simulations (left). We also consider resetting to 1 and -1 with equal probability, which gives rise to the sum of two steady states (right). This is a simple case of a resetting distribution, analysed further in section 2.2.2.

Finally, upon substituting in the values for β and γ, we obtain the solution to the steady-state equation, for $\alpha_0 = \sqrt{r/D}$,

$$p_\infty(x|x_0) = \frac{\alpha_0}{2}\exp\left(-\alpha_0|x - x_0|\right). \tag{18}$$

This agrees with the expression attained by the Fourier method in equation (11) with $x_0 = 0$. Simulations support the analytic solution that we have presented (see figure 1(a)). Note that this is a non-equilibrium steady state (NESS), since there are probability currents generated by the resetting process, with sinks at all points away from 0, and a source at 0.

2.2 Extensions to the 1D diffusion problem

We can obtain the steady-state distribution for several extensions to this problem by noting that equation (14) is a general result [4], which can be used to find the steady-state distributions for other problems under additional modelling assumptions by using a different propagator.

2.2.1 Diffusion with constant drift

In the presence of constant positive drift μ (or equivalently, a constant potential) the problem becomes one of drift-diffusion, where without resetting, the Fokker-Planck equation is

$$\frac{\partial p(x,t|x_0)}{\partial t} = D\frac{\partial^2 p(x,t|x_0)}{\partial x^2} - \mu\frac{\partial p(x,t|x_0)}{\partial x}. \tag{19}$$

This has a known propagator [21] given by

$$G_0(x,t|x_0) = \frac{1}{\sqrt{4\pi Dt}}\exp\left(-\frac{|x - x_0 - \mu t|^2}{4Dt}\right). \tag{20}$$

Using the same identity as in section 2.1.2, we obtain the steady-state distribution under resetting to $x_0 = X_r$,

$$p_\infty(x|x_0) = \frac{r}{\sqrt{4Dr+\mu^2}} \exp\left(\frac{(x-x_0)\mu}{2D} - \frac{(Dr+\mu^2/4)^{1/2}}{D}|x-x_0|\right).^{4} \tag{21}$$

This result can also be obtained by means of taking a Fourier transform and evaluating the inverse transform using Cauchy's residue theorem.

2.2.2 Resetting distribution

In addition to resetting to X_r, a fixed position, one could also extend the 1D case by allowing the particle to reset to the random variable X_r with known distribution $P(X_r)$. We modify, as in [8], the last renewal equation (13) to account for the resetting behaviour to find

$$p(x,t|x_0) = e^{-rt}G_0(x,t|x_0) + r\int_0^t d\tau e^{-r\tau}\int dX_r P(X_r)G_0(x,\tau|X_r). \tag{22}$$

As before, we consider the limiting behaviour as $t \to \infty$ and obtain the steady-state solution

$$p_\infty(x) = \int dX_r P(X_r)p_\infty(x|X_r), \tag{23}$$

where $p_\infty(x|X_r)$ is the steady-state distribution for diffusion with resetting to fixed position X_r, as in equation (18). We note that the steady-state distribution is independent of the initial position x_0.

This particular extension is of note since in many of the experimental realisations of stochastic resetting [23], the resetting distribution takes the form of a random variable rather than a fixed position.

We now compute the closed forms of p_∞ for several distributions, which may be applicable in different resetting experiments. We provide verification for the two more experimentally significant of these expressions using numerical results.

Normal distribution. In the case where $X_r \sim \mathrm{N}(\mu,\sigma^2)$, we can compute expression (23) to be

$$\begin{aligned} p_\infty(x) \ = & \frac{\alpha_0}{2}\exp\left(\frac{\alpha_0^2\sigma^2}{2}\right)\left(\exp\left(\alpha_0(\mu-x)\right)\Phi\left(\frac{x-\mu-\alpha_0\sigma^2}{\sigma}\right)\right. \\ & \left. + \exp\left(\alpha_0(x-\mu)\right)\left[1-\Phi\left(\frac{x-\mu+\alpha_0\sigma^2}{\sigma}\right)\right]\right). \end{aligned} \tag{24}$$

This case is of particular note. In an experimental setting, stochastic resetting may take the form of turning on an optical trap (well modelled by a harmonic confining potential) until the particle reaches an equilibrium state within the trap. This results in a Gaussian resetting distribution [24]. This distribution is shown, alongside our simulation of these results, in figure 2(a).

We shall now consider the closed forms of p_∞ for another two distributions. While there is currently less of an experimental basis for the consideration of these results, they are still of interest.

[4] We note that we have derived this result using the method outlined in [4], but a term in our result differs from the result presented in that paper by a factor of 2. By comparison with the results presented in [22], we suggest that our result is correct.

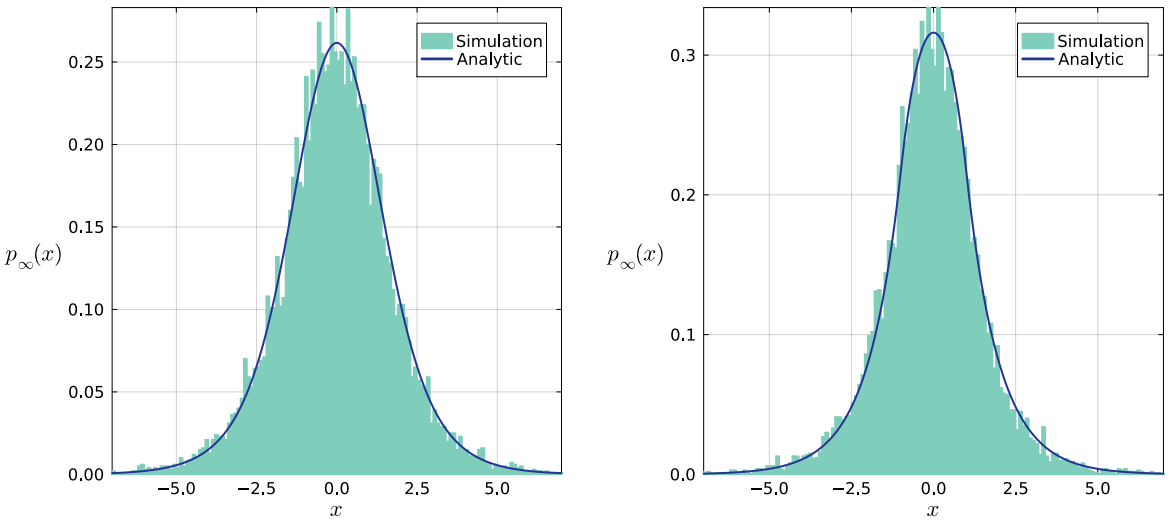

(a) $X_r \sim \mathrm{N}(0,1)$ **(b)** $X_r \sim \mathrm{Unif}([-1,1])$

Figure 2 The non-equilibrium steady state obtained for resetting according to a standard normal (left) or uniform (right) distribution. Simulated results are compared to the analytic results computed above.

Uniform distribution. In the case where $X_r \sim \mathrm{Unif}([a,b])$, we have

$$p_\infty(x) = \begin{cases} \frac{e^{\alpha_0 x}}{2(b-a)} \left[\exp\left(-\alpha_0 a\right) - \exp\left(-\alpha_0 b\right)\right], & x \le a, \\ \frac{1}{2(b-a)} \left[2 - \exp\left(\alpha_0(a-x)\right) - \exp\left(\alpha_0(x-b)\right)\right], & a < x \le b, \\ \frac{e^{-\alpha_0 x}}{2(b-a)} \left[\exp\left(\alpha_0 b\right) - \exp\left(\alpha_0 a\right)\right], & x > b. \end{cases} \tag{25}$$

This result can be seen in figure 2(b).

Exponential distribution. In the case where $X_r \sim \mathrm{Exp}(\lambda)$, $\lambda \neq \alpha_0$ we calculate expression (23) as

$$p_\infty(x) = \begin{cases} \frac{\alpha_0 \lambda}{2(\lambda+\alpha_0)} \exp\left(\alpha_0 x\right), & x \le 0, \\ \frac{\alpha_0 \lambda}{2(\lambda-\alpha_0)} \left((-\alpha_0 x) - \exp\left(-\lambda x\right)\right) + \frac{\alpha_0 \lambda}{2(\lambda+\alpha_0)} \exp\left(-\lambda x\right), & x \ge 0. \end{cases} \tag{26}$$

2.2.3 Arbitrary spatial dimension

The propagator in the case of arbitrary spatial dimension d is also known [25] to be

$$G_0(\vec{x}, t|\vec{x_0}) = \frac{1}{(4\pi D t)^{d/2}} \exp\left(-\frac{|\vec{x} - \vec{x_0}|^2}{4Dt}\right), \tag{27}$$

and we can substitute this into equation (14) to find the steady-state distribution. Again, we let $\alpha_0 = \sqrt{\frac{r}{D}}$ and now let $\nu = 1 - \frac{d}{2}$, and we obtain

$$p_\infty(\vec{x}) = \left(\frac{\alpha_0^2}{2\pi}\right)^{1-\nu} (\alpha_0 |\vec{x} - \vec{x_0}|)^\nu K_\nu(\alpha_0 |\vec{x} - \vec{x_0}|). \tag{28}$$

In the one-dimensional case ($d = 1$), one uses the same identity for $K_{1/2}$ as in section 2.1.2 to obtain equation (18). We consider the case $d = 2$ in more detail in section 3.

2.3 Optimal resetting in 1D

It has been shown that the mean first-passage time (MFPT) of a diffusive particle to reach an absorbing trap at the origin is infinite, but this becomes finite in the presence of resetting [4]. A natural question is whether the resetting process can be optimised to minimise the MFPT T of the particle.

2.3.1 Survival probability and MFPT

We first consider $Q(x,t)$, the survival probability for absorption (the probability that the particle has not been absorbed by a trap), of a particle which resets to x_0 at time t given that it started at position x. The backwards master equation which admits Q as a solution is: [12]

$$\frac{\partial Q(x,t)}{\partial t} = D\frac{\partial^2 Q(x,t)}{\partial x^2} - rQ(x,t) + rQ(x_0,t). \tag{29}$$

We find T by noting the identity

$$T(x) = -\int_0^\infty t\frac{\partial Q(x,t)}{\partial t}dt = \int_0^\infty Q(x,t)dt = \tilde{Q}(x,0), \tag{30}$$

where we integrate by parts and assume $tQ(x,t) \to \infty$ as $t \to \infty$. and we have denoted the Laplace transform with respect to t of Q by $\tilde{Q}(x,s)$.

By integrating equation (29) with respect to time, we obtain

$$-1 = D\frac{\partial^2 T(x)}{\partial x^2} - rT(x) + rT(x_0). \tag{31}$$

We solve for $T(x)$ in terms of $T(x_0)$, before applying $x = x_0$ to find an expression for $T(x_0)$. Using the boundary conditions $T(0) = 0$ and $T(x)$ is finite as $x \to \infty$, we can solve to obtain

$$T(x) = \frac{1 + rT(x_0)}{r}\Big(1 - e^{-\alpha_0 x}\Big) \implies T(x_0) = \frac{1}{r}\Big(e^{\alpha_0 x_0} - 1\Big), \tag{32}$$

where $a_0 = \sqrt{r/D}$ as before. This solution is covered in more detail in Appendix A.

2.3.2 Optimal Poissonian resetting

We note that as $r \to 0$, T diverges. This agrees with the known [4] result that the MFPT without resetting is infinite. We also see that T diverges as $r \to \infty$, suggesting the existence of a local minimum for T with respect to r. Fixing x_0 and D and considering $T = T(r)$, we find this minimum to be unique.

$$T(r) = \frac{1}{r}\Big(e^{\alpha_0 x_0} - 1\Big) \implies \frac{\partial T(r)}{\partial r} = \frac{\frac{x_0}{2}\alpha_0 e^{\alpha_0 x_0} - e^{\alpha_0 x_0} + 1}{r^2}. \tag{33}$$

Rearranging this gives us

$$1 - e^{-z} = \frac{z}{2}, \tag{34}$$

where $z \equiv \alpha_0 x_0$, which (for $z > 0$) has the unique solution $z^* \approx 1.59362$ [12]. The optimal resetting rate is then given by $r^* = (z^*)^2 D/x_0^2 \approx 2.53962 D/x_0^2$.

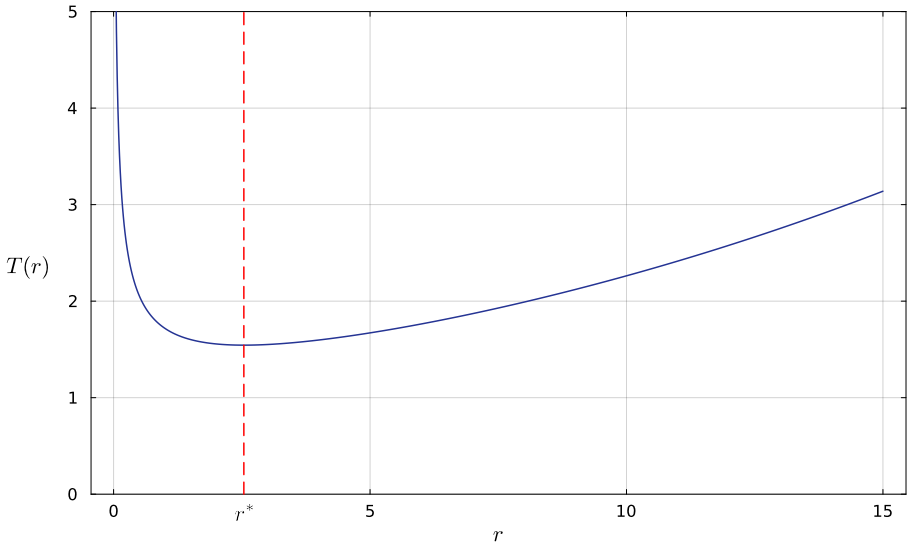

Figure 3 MFPT $T(x)$ plotted against r, with $x_0 = D = 1$. Divergence as $r \to 0$ and $r \to \infty$ suggests the existence of a minimum, which we show to be $r^* \approx 2.53962$.

2.3.3 Time-dependent resetting

We can generalise the resetting process by considering a time-dependent resetting rate $r(t)$. The approach and methods in this section are adopted from [11]. Now, we cannot write a master equation for $p(x, t|x_0)$ because we must also keep track of time since the most recent reset. The *first renewal equation* is more useful in studying the steady-state distribution of the time-dependent rate process. We first define the quantity

$$R(t) = \int_0^t d\tau\, r(\tau). \tag{35}$$

The probability of no resets up to time t is $e^{-R(t)}$ and the probability of the first reset in the interval $t \to t + dt$ is $r(t)e^{-R(t)}$. Then, for the time-dependent resetting process, the *first renewal equation* becomes

$$p(x, t|x_0) = e^{-R(t)}G(x, t|x_0) + \int_0^t d\tau \cdot r(\tau)e^{-R(\tau)}p(x, t - \tau|x_0), \tag{36}$$

where the integral is over the first resetting time τ. By taking the Laplace transform, we find

$$\tilde{p}(x, s|x_0) = \frac{\tilde{q}(x, s|x_0)}{s\tilde{H}(s)}, \tag{37}$$

where

$$\tilde{p}(x, s|x_0) = \int_0^\infty e^{-st}p(x, t|x_0)\, dt, \tag{38}$$

$$\tilde{q}(x, s|x_0) = \int_0^\infty e^{-st}e^{-R(t)}G_0(x, t|x_0)\, dt, \tag{39}$$

$$\tilde{H}(s) = \int_0^\infty e^{-st}e^{-R(t)}\, dt. \tag{40}$$

By the final value theorem, $\lim_{t\to\infty} p(x,t|x_0) = \lim_{s\to 0} s\tilde{p}(x,s|x_0)$. Hence, we consider time-dependent resetting functions $r(t)$, for which the limit exists and is non-zero. The steady-state distribution is then given by

$$p_\infty(x|x_0) = \frac{\tilde{q}(x,0|x_0)}{\tilde{H}(0)}. \tag{41}$$

From definitions (39) and (40), we see that if $\lim_{s\to 0}\tilde{H}(s) < \infty$, then $\lim_{s\to 0}\tilde{q}(x,s|x_0) < \infty$. Thus, a sufficient condition for the existence of the steady-state distribution is $\lim_{s\to 0}\tilde{H}(s) < \infty$, which implies

$$\int_0^\infty e^{-R(t)}\,dt < \infty. \tag{42}$$

Below, we study some possible choices for the time-dependent rate.

Linear rate. One choice for the resetting rate can be $r(t) = b_0 t$, where b_0 is a positive constant. This gives $R(t) = b_0 t^2/2$ which satisfies condition (42). We also obtain

$$\tilde{q}(\vec{x},s|x_0) = \int_0^\infty e^{-st}e^{-b_0t^2/2}\frac{1}{(4\pi Dt)^{d/2}}\exp\left(-\frac{|\vec{x}-\vec{x_0}|^2}{4Dt}\right)dt, \tag{43}$$

$$\tilde{H}(s) = \int_0^\infty e^{-st}e^{-b_0t^2/2}\,dt = e^{s^2/2b_0}\int_0^\infty \exp\left(-\frac{b_0}{2}(t+s/b_0)^2\right)dt = \sqrt{\frac{\pi}{2b_0}}e^{s^2/b_0}\,\mathrm{erfc}\left[\frac{s}{\sqrt{2b_0}}\right]. \tag{44}$$

Particularly, in one dimension we have

$$\begin{aligned}\tilde{q}(x,0|x_0) &= \int_0^\infty e^{-b_0t^2/2}\frac{1}{\sqrt{4\pi Dt}}\exp\left(-\frac{|x-x_0|^2}{4Dt}\right)dt \\ &= \sqrt{\frac{\pi}{2b_0}}\frac{\sqrt[4]{b_0}}{\sqrt{4\sqrt{2}\pi D}}\int_0^\infty e^{-z^2}\frac{1}{\sqrt{z}}\exp\left(-\frac{\sqrt{b_0}|x-x_0|^2}{4\sqrt{2}Dz}\right)dz.\end{aligned}$$

The steady-state distribution can thus be written as

$$p_\infty(x) = \frac{\sqrt[4]{b_0}}{\sqrt{4\sqrt{2}\pi D}}\left(\frac{d}{dl}J(l)\right)_{l=\frac{|x-x_0|\sqrt[4]{b_0}}{\sqrt{4\sqrt{2}D}}}, \tag{45}$$

$$J(l) = \int_0^\infty e^{-z^2}\,\mathrm{erf}\left(\frac{l}{\sqrt{z}}\right)dz. \tag{46}$$

Increasing, but bounded rate. We can also consider a rate function that does not increase unboundedly, such as $r(t) = b_0(\frac{1}{\varepsilon} - \frac{1}{t+\varepsilon})$, where b_0/ε is an upper bound. Thus, $R(t)$ is given by $R(t) = b_0(t/\varepsilon) - b_0\log(1+t/\varepsilon)$ and $e^{-R(t)} \to 0$ as $t\to\infty$. We calculate

$$\begin{aligned}\tilde{H}(0) &= \int_0^\infty e^{-b_0t/\varepsilon}(1+t/\varepsilon)^{b_0}\,dt, \\ &= \varepsilon\frac{e^{b_0}}{b_0}\int_{b_0}^\infty e^{-z}\left(\frac{z}{b_0}\right)^{b_0}dz = \varepsilon\exp\left(b_0-(1+b_0)\log b_0\right)\Gamma_g(1+b_0,b_0).\end{aligned}$$

where $\Gamma_g(u,v) = \int_v^\infty w^{u-1}e^{-w}\,dw$ is an incomplete Gamma function. In the one-dimensional case, using the variable substitution $z = t/\varepsilon$

$$\tilde{q}(x,0|x_0) = \int_0^\infty e^{-b_0 t/\varepsilon}\frac{1}{\sqrt{4\pi D t}}\exp\left(-\frac{|x-x_0|^2}{4Dt}\right)dt = \frac{\sqrt{\varepsilon}}{4\sqrt{D}}\left(\frac{d}{dl}\mathfrak{J}_{b_0}(l)\right)_{l=\frac{|x-x_0|}{\sqrt{4D\varepsilon}}}, \tag{47}$$

where

$$\mathfrak{J}_{b_0}(l) = \int_0^\infty e^{-b_0 z}(1+z)^{b_0}\text{erf}\left(\frac{l}{\sqrt{z}}\right)dz, \tag{48}$$

Therefore, the steady-state distribution in one dimension is given by

$$p_\infty(x) = \frac{\exp\left((1+b_0)\log b_0 - b_0\right)}{\Gamma_g(1+b_0,b_0)}\frac{1}{4\sqrt{D\varepsilon}}\left(\frac{d}{dl}\mathfrak{J}_{b_0}(l)\right)_{l=\frac{|x-x_0|}{\sqrt{4D\varepsilon}}}. \tag{49}$$

Rates decreasing as a power law. We now consider decreasing time-dependent resetting functions and require the rate to decrease sufficiently slowly to satisfy condition (42). We consider $r(t) \sim b_0/t^\theta$, with θ a real constant.

In the case $\theta < 1$, we take $r(t) = b_0/t^\theta, t > 0$. Then $R(t) = b_0 t^{1-\theta}/(1-\theta)$, and

$$\tilde{H}(0) = \int_0^\infty e^{-R(t)}\,dt = \frac{(1-\theta)^{\theta/(1-\theta)}}{b_0^{1/(1-\theta)}}\Gamma\left(\frac{1}{1-\theta}\right) < \infty. \tag{50}$$

In the case $\theta > 1$, we take $r(t) = b_0/(t+\varepsilon)^\theta$ to ensure the convergence of $R(t)$. Then $R(t) \to \frac{b_0}{(\theta-1)\varepsilon^{\theta-1}}$ as $t \to \infty$. Thus $e^{-R(t)} \to$ constant > 0 and therefore condition (42) is not satisfied. Moreover, we can show that $\tilde{H}(s) \sim 1/s$ and $\tilde{Q}(x,s|x_0) \sim s^{d/2-1}$ for $s \to 0$:

$$\lim_{s\to 0} s\tilde{H}(s) = \lim_{t\to\infty} e^{-R(t)} = \exp\left(\frac{b_0}{\theta-1}\varepsilon^{\theta-1}\right),$$

$$\lim_{s\to 0} s^{1-d/2}\tilde{q}(x,s|x_0) = \lim_{t\to\infty} t^{d/2}Q(x,t|x_0) = \frac{1}{(4\pi D)^{d/2}}\exp\left(\frac{b_0}{\theta-1}\varepsilon^{\theta-1}\right),$$

where we have used the final value theorem. Hence, $\frac{\tilde{q}(x,s|x_0)}{\tilde{H}(s)} \to 0$ as $s \to 0$. Thus, there does not exist a steady state for arbitrary dimension d.

In the case $\theta = 1$, we take $r(t) = b_0/(t+\varepsilon)$, for which $e^{-R(t)} = (\frac{\varepsilon}{t+\varepsilon})^{b_0}$. For $b_0 \le 1, \tilde{H}(s)$ diverges as $s \to 0$ and for $b_0 > 1, \tilde{H}(s)$ converges as $s \to 0$. Hence, for $b_0 > 1$,

$$p_\infty(\vec{x}) = \frac{b_0-1}{\varepsilon}\int_0^\infty\left(\frac{\varepsilon}{t+\varepsilon}\right)^{b_0}\frac{1}{(4\pi D t)^{d/2}}\exp\left(-\frac{|\vec{x}-\vec{x}_0|^2}{4Dt}\right)dt. \tag{51}$$

Next we consider the survival probability and MFPT under time-dependent resetting. It is a well-known result [26] that the survival probability, $Q_0(x_0,t)$, of a free diffusive particle (without resetting), given that it starts at x_0 is

$$Q_0(x_0,t) = \text{erf}\left[\frac{x_0}{\sqrt{4Dt}}\right]. \tag{52}$$

Let $Q_r(x_0, X_r, t)$ denote the survival probability under resetting of a particle which starts at x_0 and undergoes resetting to X_r until time t. For convenience we assume $X_r = x_0$. Thus, the first renewal equation becomes

$$Q_r(x_0, x_0, t) = e^{-R(t)}Q_0(x_0, t) + \int_0^t d\tau_f\, r(\tau_f)e^{-R(\tau_f)}Q_0(x_0, \tau_f)Q_r(x_0, x_0, t - \tau_f). \tag{53}$$

The first term represents the trajectories in which there has been no resetting or absorption by the origin until time t. The second term sums over the first resetting time τ_f, where the quantity $r(\tau_f)e^{-R(\tau_f)}Q_0(x_0, \tau_f)$ gives the survival probability of resetting at time τ_f and the probability that a reset occurs between τ_f and $\tau_f + d\tau_f$ and the quantity $Q_r(x_0, x_0, t - \tau_f)$ represents the probability of no absorption occurring between times τ_f and t. Taking the Laplace transform of (53) and rearranging, we obtain

$$\tilde{Q}_r(x_0, x_0, s) = \frac{\tilde{q_r}(x_0, s)}{s\tilde{q_r}(x_0, s) - \tilde{k_r}(x_0, s)}, \tag{54}$$

where we have defined

$$\tilde{q_r}(x_0, s) = \int_0^\infty dt\, e^{-st}e^{-R(t)}Q_0(x_0, t), \tag{55}$$

$$\tilde{k_r}(x_0, s) = \int_0^\infty dt\, e^{-st}e^{-R(t)}\frac{d}{dt}Q_0(x_0, t). \tag{56}$$

Substituting to equation (30) we obtain

$$T(x_0) = -\frac{\tilde{q_r}(x_0, 0)}{\tilde{k_r}(x_0, 0)}. \tag{57}$$

After some algebraic manipulation, we can re-express $T(x_0)$ as

$$T(x_0) = -4I(\beta)\left(\frac{d^2I}{d\beta^2}\right)^{-1}, \text{ with } \beta = \frac{x_0}{\sqrt{4D}} \text{ and } I(\beta) = \int_0^\infty dt\, e^{-R(t)}\text{erf}\left(\frac{\beta}{\sqrt{t}}\right). \tag{58}$$

In the linear case, $r(t) = b_0 t$, using the variable change $z = \sqrt{b_0/2}t$, we show that

$$I(\beta) = \sqrt{\frac{2}{b_0}}J\left(\beta\sqrt[4]{\frac{b_0}{2}}\right), \tag{59}$$

where $J(l)$ is as defined as before, in equation (46).

In the case $r(t) = b_0(1/\varepsilon - 1/(t + \varepsilon))$, using the variable change $t = \varepsilon z$, we show that

$$I(\beta) = \varepsilon\mathfrak{J}_{b_0}(\beta/\sqrt{\varepsilon}), \tag{60}$$

where $\mathfrak{J}_{b_0}$ is as in equation (48). In figure 4, we plot the MFPT as a function of b_0 for fixed ε and $x_0 = D = 1$. We observe a range of values of b_0 for which $T(x_0)$ is smaller than the minimum possible MFPT found using a constant rate.

Optimal resetting rate function The question that arises is whether we can find an optimal $r(t)$ that minimizes the MFPT. We take the functional derivative of equation (30) with respect to $r(t)$ at t'

$$\frac{\delta T(x_0)}{\delta r(t')} = \frac{1}{\tilde{k_r}(x_0, 0)}\int_{t'}^\infty dt\, e^{-R(t)}Q_0(x_0, t) - \frac{\tilde{q_r}(x_0, 0)}{[\tilde{k_r}(x_0, 0)]^2}\int_{t'}^\infty dt\, e^{-R(t)}\frac{\partial Q_0(x_0, t)}{\partial t} \tag{61}$$

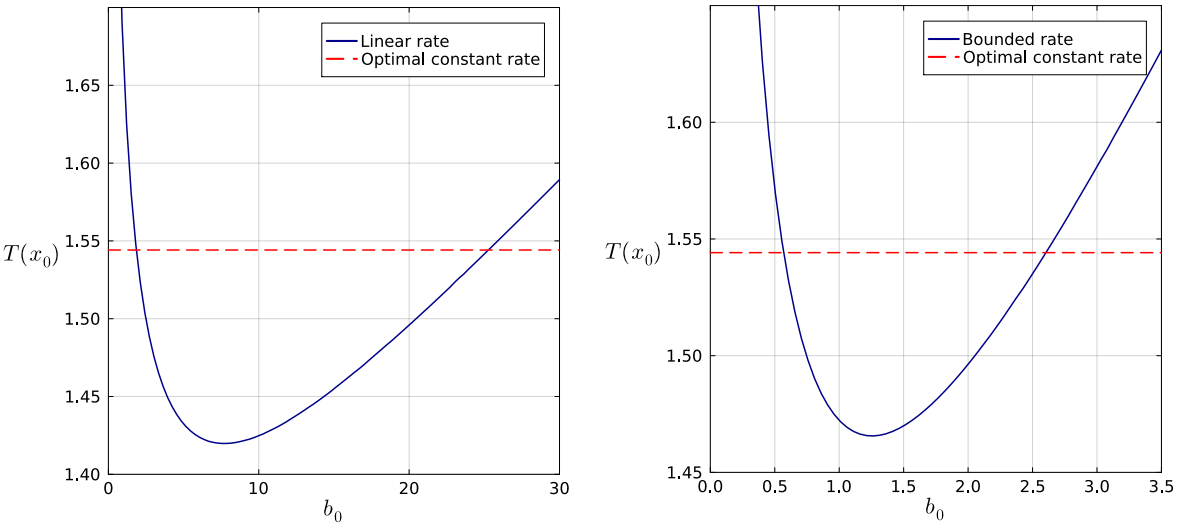

(a) $r(t) = b_0 t$ **(b)** $r(t) = b_0(\frac{1}{\varepsilon} - \frac{1}{t+\varepsilon})$

Figure 4 Plot of MFPT as a function of b_0 for the rate functions (a) $r(t) = b_0 t$ and (b) $r(t) = b_0(\frac{1}{\varepsilon} - \frac{1}{t+\varepsilon})$. The diffusion constant is set to $D = 1$, the resetting and initial positions to $X_r = x_0 = 1$ and $\varepsilon = 0.25$. The main observation is that for a range of values of b_0, the MFPT is smaller than the one achieved for the optimum constant rate found in 2.3.2 and plotted with the red dashed line.

Setting the right-hand side equal to zero, we find that the optimal time-dependent rate function must satisfy

$$e^{-R(t')}\left[\tilde{k}_r(x_0,0)Q_0(x_0,t') - \tilde{q}_r(x_0,0)\frac{\partial Q_0(x_0,t)}{\partial t}\bigg|_{t=t'}\right] = 0, \tag{62}$$

for all $t = t'$. Rearranging, we find that

$$\frac{1}{Q_0(x_0,t')}\frac{\partial Q_0(x_0,t')}{\partial t}\bigg|_{t=t'} = \frac{\tilde{k}_r(x_0,0)}{\tilde{q}_r(x_0,0)}, \tag{63}$$

which is not satisfied for all t since the right-hand side is constant but the left-hand side is not. Since the optimal resetting function does not minimise the MFPT everywhere, it must involve values at the boundary of the rate space, i.e. $r = 0$ and $r \to \infty$. Hence, we investigate a conjectured form of $r(t)$

$$r(t) = \begin{cases} 0, & t < t^*, \\ \infty, & t \geq t^*. \end{cases} \tag{64}$$

In this form, the particle does not reset until time t^* and then resets immediately. For this time-dependent rate we have

$$T(x_0) = \frac{\int_0^{t^*} dt\, Q_0(x_0,t)}{1 - Q_0(x_0,t^*)}. \tag{65}$$

Setting the derivative of T with respect to t^* to zero yields the condition

$$\frac{\int_0^{t^*} dt\, Q_0(x_0,t)}{1 - Q_0(x_0,t^*)} = -\frac{Q_0(x_0,t^*)}{\frac{\partial Q_0(x_0,t)}{\partial t}|_{t=t^*}}. \tag{66}$$

We can write the above in terms of $z = t/\beta^2$, where β is as previously and, using equation (52), we find that

$$\frac{\int_0^{z^*} dz\, \text{erf}(1/\sqrt{z})}{1 - \text{erf}(1/\sqrt{z^*})} = \sqrt{\pi}(z^*)^{3/2} e^{1/z} \text{erf}\left(\frac{1}{\sqrt{z^*}}\right). \tag{67}$$

The equation can be solved numerically to find $z^* \approx 1.8340111$ [11]. Substituting $t^* = z^* x_0^2/(4D)$ into equation (65) we find the optimum MFPT to be $T(x_0) = 5.34354...x_0^2/(4D)$, which is smaller than the minimum MFPT that we found for a constant resetting rate in section 2.3.1.

2.3.4 Space-dependent resetting

In this subsection, we consider a space-dependent resetting rate $r(x)$. The master equation (as given in [12]) is

$$\frac{\partial p(x,t|x_0)}{\partial t} = D\frac{\partial^2 p(x,t|x_0)}{\partial x^2} - r(x)p(x,t|x_0) + \int dx'\, r(x')p(x',t|x_0)\,\delta(x - x_0). \tag{68}$$

Taking the limit $t \to \infty$, we have that the steady-state distribution $p_\infty(x|x_0)$ satisfies

$$D\frac{\partial^2 p_\infty(x|x_0)}{\partial x^2} - r(x)p_\infty(x|x_0) = -\int dx'\, r(x')p_\infty(x'|x_0)\delta(x - x_0). \tag{69}$$

The equation for the mean first-passage time in equation (31) now reads

$$-1 = D\frac{\partial^2 T(x)}{\partial x^2} - r(x)T(x) + r(x)T(x_0). \tag{70}$$

for some constant a.

Generally, it is difficult to calculate the steady-state distribution for arbitrary $r(x)$. Therefore, we consider the simple case of a resetting rate of the form

$$r(x) = \begin{cases} 0, & |x - x_0| < a \\ r, & |x - x_0| \geq a. \end{cases} \tag{71}$$

Hence, we obtain the that master equation is

$$\frac{\partial p(x,t|x_0)}{\partial t} = \begin{cases} D\frac{\partial^2 p(x,t|x_0)}{\partial x^2} + \int dx'\, rp(x',t|x_0)\Theta(|x - x_0| - a)\,\delta(x - x_0), & |x - x_0| < a \\ D\frac{\partial^2 p(x,t|x_0)}{\partial x^2} - rp(x,t|x_0), & |x - x_0| \geq a. \end{cases} \tag{72}$$

with initial condition $p(x, 0|x_0) = \delta(x - x_0)$.

In order to find the steady-state distribution, we make use of the Green's function method, as in section 2.1.2. Taking the limit $t \to \infty$, we find $D\frac{\partial^2 p_\infty(x|x_0)}{\partial x^2} = 0$, for $0 < |x - x_0| < a$, and $D\frac{\partial^2 p_\infty(x|x_0)}{\partial x^2} = p_\infty(x|x_0)$ for $|x - x_0|$. By the expected symmetry of the solution about $x = x_0$, we obtain

$$p_\infty(x|x_0) = \begin{cases} C - B(|x - x_0| - a), & |x - x_0| < a. \\ A\text{exp}(-\alpha_0(|x - x_0| - a)), & |x - x_0| \geq a \end{cases} \tag{73}$$

Using the continuity of the density and its first derivative at $|x - x_0| = a$, we find that $A = C$ and $B = \alpha_0 A$. By setting the integral of $p_\infty(x|x_0)$ equal to 1, we obtain $A = \frac{\alpha_0}{2+2a\alpha_0+a^2\alpha_0^2}$.

We now consider an absorbing target at the origin and assume that $x_0 > 0$. Equation (70) reads

$$-1 = \begin{cases} D\frac{\partial^2 T(x)}{x^2}, & |x - x_0| < a. \\ D\frac{\partial^2 T(x)}{x^2} - rT(x) + rT(x_0), & |x - x_0| \geq a. \end{cases} \tag{74}$$

Then, the general equation is given by

$$T(x) = \begin{cases} Ax + B - x^2/(2D), & |x - x_0| < a, \\ 1/r + T(x_0) + Ee^{-\alpha_0 x} + Fe^{\alpha_0 x}, & x \leq x_0 + a, \\ 1/r + T(x_0) + Ce^{-\alpha_0(x - x_0 - a)}, & x \geq x_0 + a. \end{cases} \tag{75}$$

To find the constants, we use the continuity of $T(x)$ and $T'(x)$ at $|x - x_0| = a$ and the boundary condition $T(0) = 0$. After some algebraic manipulations, we find, as in [12],

$$T(x_0) = \frac{1}{r(1 + a\alpha_0)} \Bigg[\cosh(\alpha_0(x_0 - a)) \left(1 + 2a\alpha_0 + \frac{3a^2\alpha_0^2}{2} + a^3\alpha_0^3 \right) + \sinh(\alpha_0(x_0 - a) \cosh(\alpha_0(x_0 - a)) \left(1 + 2a\alpha_0 + \frac{3a^2\alpha_0^2}{2} \right) \Bigg] - \frac{1}{r}. \tag{76}$$

We now substitute the parameters $z = \alpha_0 x_0$ and $y = \alpha_0 a$. We require that y satisfies $0 \leq y \leq z$, so we find that $\frac{dT}{dy}|_{y=z} = \frac{2y^2 + y^3}{2r(1+y)^2} > 0$, and we conclude that T achieves a minimum at either $y = 0$ or some point in $(0, z)$. The condition $\frac{dT}{dy} = 0$ reduces to $\tanh(z - y) = \frac{2+y}{4+5y+2y^2}$, from which we observe that if $\tanh z > 1/2 \Leftrightarrow z > (\log 3)/2$, the minimum is attained at some $y = y^* > 0$. Otherwise, it is attained at $y = 0$. Therefore, if $z < (\log 3)/2$, the presence of the non-resetting window around x_0 does not reduce the mean first-passage time.

The relevant optimization problem is finding the optimal resetting rate $r(|x - x_0|)$ (a function of the distance $|x - x_0|$ from the resetting site) which minimises $T(x_0)$. This remains an open problem [12].

3 Diffusion with resetting in 2D

We have seen in section 2.2.3 that one can use resetting for a diffusive particle in higher dimensions. In this section, we focus on the two-dimensional case, since this provides a more interesting framework for our application to bacterial motion. For this discussion, we consider the diffusive motion of a particle around $\mathbb{R}^2$ under stochastic resetting.

3.1 Renewal approach in 2D

The Fokker-Planck equation for the 2D diffusive problem is a direct extension of the 1D case, given by equation (1a), replacing the spatial second derivative with the Laplacian [25]. Therefore, we can write down that the master equation is

$$\frac{\partial p(\vec{x}, t)}{\partial t} = D\nabla^2 p(\vec{x}, t) - rp(\vec{x}, t) + r\delta^2(\vec{x} - \vec{x}_0), \tag{77}$$

where ∇^2 denotes the 2D Laplacian, and $\delta^2(\vec{x})$ is the 2-dimensional δ-function. The boundary condition $p(\vec{x}, 0) = \delta^2(\vec{x} - \vec{x}_0)$ also persists into the 2-dimensional case.

The key result that we have derived to this end is equation (28), where $d = 2$, with $\nu = 0$. Therefore, the renewal approach to solving the steady-state 2D diffusion equation gives

$$p_\infty(\vec{x}) = \frac{\alpha_0^2}{2\pi} K_0(\alpha_0|\vec{x} - \vec{x}_0|), \tag{78}$$

where, as before, $\alpha_0 = \sqrt{r/D}$ and $K_0(x)$ is the modified Bessel function of the second kind of order 0, which is known [27] to be

$$K_0(x) = \int_0^\infty \cos(x\text{sinh}t)dt = \int_0^\infty \frac{\cos(xt)}{\sqrt{t^2+1}}dt. \tag{79}$$

We can therefore express the 2D steady-state solution to the diffusion problem under resetting as

$$p_\infty(\vec{x}) = \frac{\alpha_0^2}{2\pi} \int_0^\infty \frac{\cos(\alpha_0|\vec{x} - \vec{x}_0|t)}{\sqrt{t^2+1}}dt. \tag{80}$$

It is noteworthy that the time-dependent solution can be recovered simply by the substitution of the 2D diffusive propagator into the last renewal equation, as outlined in section 2.2.3. Hence the solution given by equation (80) represents the steady-state limit of this equation. For completeness, we present the time-dependent solution in equation (81)

$$p(\vec{x}, t) = \frac{e^{-rt}}{4\pi Dt} \exp\left(-\frac{|\vec{x} - \vec{x}_0|^2}{4Dt}\right) + r\int_0^t d\tau \frac{e^{-r\tau}}{4\pi D\tau} \exp\left(-\frac{|\vec{x} - \vec{x}_0|^2}{4D\tau}\right). \tag{81}$$

3.2 Extending the 2D diffusion problem to one of drift-diffusion

We consider a constant drift in an arbitrary direction, $\vec{\mu} = (\mu_1, \mu_2)^T$. The Fokker-Planck equation for drift-diffusion without resetting, as in [28], is

$$\frac{\partial p(\vec{x}, t|\vec{x_0})}{\partial t} = D\nabla^2 p(\vec{x}, t|\vec{x_0}) - \vec{\mu} \cdot \nabla p(\vec{x}, t|\vec{x_0}), \tag{82}$$

with initial condition $p(\vec{x}, 0|\vec{x_0}) = \delta^2(\vec{x} - \vec{x_0})$ (where $\vec{x} \equiv (x, y)^T$). Taking Fourier transforms, we obtain the equation

$$\frac{\partial}{\partial t}\hat{p}(\omega_x, \omega_y, t) = -D(\omega_x^2 + \omega_y^2)\hat{p}(\omega_x, \omega_y, t) - i(\mu_1\omega_x + \mu_2\omega_y)\hat{p}(\omega_x, \omega_y, t). \tag{83}$$

We use the initial condition to solve the differential equation and find that

$$\hat{p}(\omega_x, \omega_y, t) = \exp\left[-i(\omega_x x_0 + \omega_y y_0)\right] \exp[-Dt(\omega_x^2 + \omega_y^2) - it(\mu_1\omega_x + \mu_2\omega_y)]. \tag{84}$$

We compute the inverse Fourier transform by making the variable substitutions $x = \sqrt{Dt}x' + \mu_1 t + x_0$, $y = \sqrt{Dt}y' + \mu_2 t + y_0$, and obtain

$$p(\vec{x}, t|\vec{x_0}) = \frac{1}{4\pi Dt} \exp\left(-\frac{|\vec{x} - \vec{x_0} - \vec{\mu}t|^2}{4Dt}\right). \tag{85}$$

Substituting this into the last renewal equation, given in equation (13) and taking the limit $t \to \infty$, we find that the steady-state distribution for drift-diffusion with resetting to the initial position $X_r = x_0$ is

$$p_\infty(\vec{x}|\vec{x_0}) = r\int_0^\infty d\tau \frac{e^{-r\tau}}{4\pi D\tau} \exp\left(-\frac{|\vec{x} - \vec{x_0} - \vec{\mu}\tau|^2}{4D\tau}\right). \tag{86}$$

3.3 Asymptotic behaviour of a particle diffusing to a single absorbing trap

We now consider a purely diffusive particle in the presence of an absorbing circle of radius a centred at the origin. The particle starts at position $|\vec{x_0}| > a$ and resets to position $\vec{X}_r$ with constant rate r. Adapting equation (29) to two dimensions yields

$$\frac{\partial Q(\vec{x_0},t)}{\partial t} = D\nabla^2 Q(\vec{x_0},t) - rQ(\vec{x_0},t) + rQ(\vec{X}_r,t), \tag{87}$$

with boundary condition $Q(|\vec{x_0}| = a, t) = 0$ and initial condition $Q(\vec{x_0}, 0) = 1$ for $|\vec{x}| > a$. Taking the Laplace transform, we obtain

$$D\nabla^2 \tilde{Q}(\vec{x_0},s) - (r+s)\tilde{Q}(\vec{x_0},s) = -1 - rQ(\vec{X}_r,s). \tag{88}$$

The solution to the homogeneous equation that is symmetric about the origin and does not diverge as $|\vec{x_0}| \to \infty$ is known and given in [25] to be

$$\tilde{Q}_{\text{hom}}(\vec{x_0},s) = K_0(\alpha|\vec{x_0}|), \tag{89}$$

where $\alpha \equiv \alpha(s) = \sqrt{(r+s)/D}$ and $\tilde{Q}_{\text{hom}}$ denotes the Laplace transform of the solution to the homogeneous equation. Thus, the solution to equation (88) is given by $\tilde{Q}(\vec{x_0},s) = B\tilde{Q}_{\text{hom}}(\vec{x_0},s) + C$, where B and C are independent of $|\vec{x_0}|$. Using the boundary condition, we obtain $C = -BK_0(\alpha a)$. Upon substitution into equation (89), we find

$$B = -\frac{1}{sK_0(\alpha a) + rK_0(\alpha|\vec{X}_r|)}, \tag{90}$$

$$\tilde{Q}(\vec{x_0},s) = \frac{K_0(\alpha a) - K_0(\alpha|\vec{x_0}|)}{sK_0(\alpha a) + rK_0(\alpha|\vec{X}_r|)}. \tag{91}$$

If we take $\vec{x_0} = \vec{X}_r$ for the sake of simplicity and denote $|\vec{X}_r|$ by R_r, we uncover

$$\tilde{Q}(R_r,s) = \frac{K_0(\alpha a) - K_0(\alpha R_r)}{sK_0(\alpha a) + rK_0(\alpha R_r)}. \tag{92}$$

It is difficult to find the inverse Laplace transform for all parameters, but we can deduce the long-time asymptotics of the survival probability. For a fixed r,

$$Q(R_r,t) = \frac{1}{2\pi i}\int_C ds\, e^{st}\frac{K_0(\alpha a) - K_0(\alpha R_r)}{sK_0(\alpha a) + rK_0(\alpha R_r)} = \frac{1}{2\pi i}\int_C ds\, \frac{e^{st}}{r}\left(\frac{r+g(s)}{s-g(s)}\right), \tag{93}$$

where C is the Bromwich Contour to the right of any singularities in the complex s-plane, and

$$g(s) = -r\frac{K_0(\alpha(s)R_r)}{K_0(\alpha(s)a)}. \tag{94}$$

The integrand has a simple pole at $s = s_0$ which satisfies $g(s_0) = s_0$, and a branch point at $s = -r$ since $\alpha(-r) = 0$. Using Cauchy's residue theorem, we find, as in [25], that for large t,

$$Q(R_r,t) \simeq \frac{e^{s_0 t}}{r}\frac{r+s_0}{1-g'(s_0)}. \tag{95}$$

By introducing $\eta = \alpha_0 R_r, \varepsilon = a/R_r$, and performing some algebraic manipulation [25], in which we make the substitution $s_0 = r(u_0 - 1)$, for some $u_0 \in (0,1)$, we obtain that the asymptotic behaviour of equation (95) is

$$Q(R_r,t) \sim \exp\left(-rt\varepsilon^{1/2}e^{-\eta(1-\varepsilon)}\right). \tag{96}$$

This is a Gumbel distribution, which arises as the CDF of a maximum of independent random variables satisfying the decay condition given by [25]. This is result that we expect, since a particle that has survived by time t must have survive N resets. Thus, we are bounded by N searches away from our trapping circle. This is analogous to the extreme value statistics in which the Gumbel distribution is observed.

We now consider the mean first-passage time to the circular trap, which we understand as the average time for a particle to be absorbed. We consider absorption to be any instance in which the particle hits the boundary of the circle at distance a from the origin. Using equation (30), we have

$$T(R_r) = \frac{1}{r}\left(\frac{K_0(\alpha_0 a)}{K_0(\alpha_0 R_r)} - 1\right). \tag{97}$$

Using the substitutions with η and ε, as above, we obtain that

$$T(R_r) = \frac{1}{\eta^2}\left(\frac{K_0(\varepsilon\eta)}{K_0(\eta)} - 1\right)\frac{R_r^2}{D}. \tag{98}$$

We note that T is finite for positive r and that, using the small argument expansion $K_0(x) \simeq \log(x/2) - \gamma_E$, T diverges according to $T \sim 1/(r|\log(r)|)$ as $r \to 0$, where γ_E is the Euler constant. In the limit $r \to \infty$, which is correspondent to $\eta \to \infty$ under our substitutions, we use the asymptotic behaviour, given in [25] to be

$$K_0(x) \simeq \sqrt{\frac{\pi}{2x}}e^{-x}[1 + O(1/x)], \tag{99}$$

to find that T diverges according to $T \sim e^{\eta(1-\varepsilon)}/\eta$.

Finally, we consider the behaviour of the system in the limit $\varepsilon \to 0$, which we understand as the case in which the initial distance between the particle and the target is much larger than the target itself. Using the small argument expansion presented above, we find that, for small ε,

$$T \sim \frac{-\log(\varepsilon)}{\eta^2 K_0(\eta)}\frac{R_r^2}{D}. \tag{100}$$

We minimize T by solving $\frac{dT}{d\eta} = 0$. We assume that $\eta = \eta^*$ minimises T. Then, η^* satisfies

$$2K_0(\eta^*) - \eta^* K_1(\eta^*) = 0, \tag{101}$$

where we have used an identity given in [20]: $K_0'(\eta) = -K_1(\eta)$.

3.4 Asymptotics in a sea of traps

A common scenario in chemistry [13] is the diffusion of a particle (or density of particles) in $\mathbb{R}^2$ against a sea of traps. We focus on the case of stationary traps and reference some results for the case where traps are also diffusive.

We consider a single particle which diffuses in $\mathbb{R}^2$ with diffusion constant D, against a background of point 'traps'. The particle is absorbed immediately if it comes within radius a of a trap. We refer to the survival probability of this single particle as $Q_0(t)$, but note that this is analogous to the proportion of particles remaining from some initial density at time t, as is often analysed in literature [13].

3.4.1 Poisson-distributed traps

We consider the case in which traps are distributed according to a Poisson distribution in a subspace of $\mathbb{R}^d$. It is known [13] that for large t, and for some constant λ_d,

$$Q_0(t) \sim \exp\left(-\lambda_d t^{\frac{d}{d+2}}\right). \tag{102}$$

This result can be obtained using the asymptotic properties of the *Wiener Sausage*. For a particle undergoing Brownian motion at position $x(t)$ at time t, the *Wiener Sausage* of radius δ until time t is given by

$$W_x^\delta(t) = \bigcup_{\tau\in[0,t]} B_\delta(x(\tau)). \tag{103}$$

In the case of $d = 2$, this is equal to the area visited by a Brownian particle of size δ until time t. We note that the survival probability, $Q_0(t)$, of our diffusive particle is exactly the probability that no trap has come within distance a of our particle, which is equivalent to the area W_x^a being trap-free. We assume that our traps are Poisson-distributed, i.e. the probability of the Wiener sausage being trap-free is given by

$$Q_0^*(t) = \mathbb{P}(\text{No traps encountered}) = \exp(-\rho|W_x^a(t)|), \tag{104}$$

where ρ is a fixed trap density. Here, $Q_0^*(t)$ is the probability that a given sausage is trap-free, but we shall consider the average across all Brownian paths, denoted by E_x. Employing a result from Donsker and Varadhan [29], we have that

$$\lim_{t\to\infty} \frac{1}{t^{1/2}} \log E_x[\exp(-\rho|W_x^a(t)|)] = -2\sqrt{\rho\gamma}. \tag{105}$$

where γ is a constant.

For large t, rearranging 105 gives result (102), in which decay is slower than exponential. This slightly unexpected [30] behaviour has been attributed to the existence of a few large trap-free regions [14]. This has been justified by bounding below by the subset of motions in which a large trap-free sphere surrounds the origin [14]. Due to this, we might not expect that the stochastic resetting described above would change this behaviour, as the trap-free sphere would remain. However, one could conceive that resetting stochastically to a random position would recover the expected exponential decay, preventing a particle from existing in a trap-free region for long periods of time.

In fact, we can use a bounding argument to show that this is the case. We consider $\tilde{Q}(t)$, the Laplace transform of the survival probability at time t, in which we consider that the particle is absorbed only when it resets directly into a trap. Clearly $Q_r(t) < \tilde{Q}(t)$, since we remove the source of absorption in which a particle diffuses into a trap. We obviously have

$$\begin{aligned}\tilde{Q}(t) &= \mathbb{P}(\text{No resets}) + \mathbb{P}(1\text{ reset})\cdot\mathbb{P}(\text{Survive a reset}) + \dots \\ &= \sum_{n=0}^{\infty} \mathbb{P}(\text{n resets})\cdot\mathbb{P}(\text{Survive a reset})^n.\end{aligned} \tag{106}$$

Since they occur at a constant rate, the number of resets before time t follows a Poisson distribution with rate parameter rt, and the probability of surviving a reset is the probability that the ball $B_a(\vec{X}_r)$ is trap-free. Thus, we obtain

$$\tilde{Q}(t) = \sum_{n=0}^{\infty} \frac{(rt)^n}{n!} e^{-rt}\cdot\left(e^{-\rho\pi a^2}\right)^n = \exp\left(-\left(1-e^{-\rho\pi a^2}\right)rt\right), \tag{107}$$

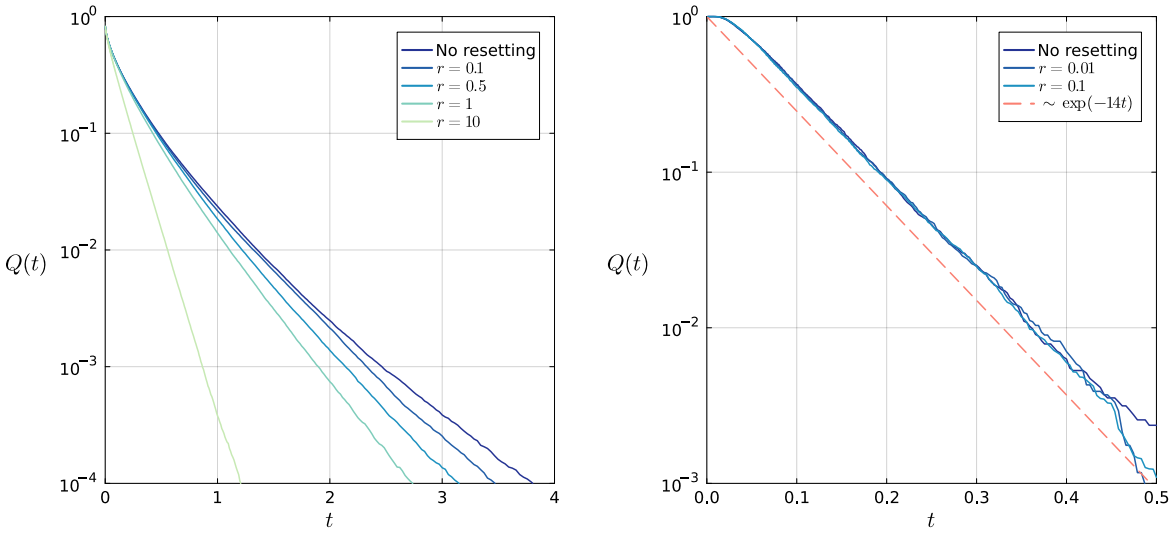

(a) Poisson-distributed traps.

(b) Integer-coordinate traps.

Figure 5 10^5 trap realisations, each with 10 particles simulated. For Poisson-distributed traps (left), we note that the decay becomes significantly faster even for small values of r, and we compare these with the lower bound from [14]. With integer-coordinate traps (right), we observe exponential decay even without resetting, and introducing a small resetting rate only makes a small change.

which clearly exhibits exponential decay. As this is an upper bound for Q_r, we have that resetting maintains the exponential decay since we include the probability of resetting directly into a trap. This is supported by numerical simulations, which show faster decay in the resetting case, with even low resetting rates having a drastic effect on the decay rate. This can be observed in figure 5.

We later examine the short-term properties and contrast them with the corresponding run-and-tumble particles in section 5.3

3.4.2 Periodic trap distributions

Since the slow decay is attributed to rare, but large, trap-free regions, another intuitive approach could be to use a more regular distribution of traps. For example, placing traps at integer coordinates only would not permit such large trap-free areas. As in the previous case, we simulate numerically, and observe roughly exponential decay, with variations in r making little difference. This is shown alongside the previous result in figure 5. However, an intuitive result is that for large values of r, the particle resets before it can encounter one of the traps. Therefore, we expect a vastly different result from those presented in figure 5.

The above is an example of a hyperuniform point pattern [31] - in particular, a periodic one. An interesting extension would be whether or not these decay properties also apply to general hyperuniform point processes, and to obtain experimental results for some non-periodic processes (of which only a few are known).

4 Run-and-tumble particles with resetting in 1D

We now consider run-and-tumble particles under resetting. Run-and-tumble motion is a process in which a particle 'runs' (moves in a single direction) and 'tumbles' (changes direction instantaneously) between runs. Bacteria such as Escherichia coli (E. coli) are commonly modelled as run-and-tumble particles (RTPs) [17], and we compare and contrast their behaviours with particles under diffusion. In our model of run-and-tumble motion, we only consider the case in which runs are purely ballistic, so we treat any drift in runs as negligible.

4.1 Run-and-tumble without resetting

Here, and in subsequent sections, we denote by v_0 the constant run speed of an RTP and by γ the tumbling rate. For $d = 1$, an RTP is modelled as moving along the real line with speed v_0 and reversing directions instantaneously at rate γ. In this subsection, we follow the approach in [18].

We can represent the 1D run-and-tumble model without resetting using a pair of Fokker-Planck equations.

$$\frac{\partial P_+(x,t)}{\partial t} = -v_0 \frac{\partial P_+(x,t)}{\partial x} - \gamma P_+(x,t) + \gamma P_-(x,t), \tag{108a}$$

$$\frac{\partial P_-(x,t)}{\partial t} = +v_0 \frac{\partial P_-(x,t)}{\partial x} - \gamma P_-(x,t) + \gamma P_+(x,t), \tag{108b}$$

where $P_+(x,t)$ represents the probability density of a particle having velocity $+v_0$ at position x and time t (and equivalently for $P_-(x,t)$).

Taking the Laplace transforms of equations (108a) and (108b), we obtain

$$-P_+(x,0) + v_0 \frac{\partial \tilde{P}_+(x,s)}{\partial x} + (s+\gamma)\tilde{P}_+(x,s) - \gamma \tilde{P}_-(x,s) = 0, \tag{109a}$$

$$-P_-(x,0) - v_0 \frac{\partial \tilde{P}_+(x,s)}{\partial x} + (s+\gamma)\tilde{P}_-(x,s) - \gamma \tilde{P}_+(x,s) = 0. \tag{109b}$$

Using the symmetric initial conditions $P_+(x,0) = P_-(x,0) = \frac{1}{2}\delta(x)$, we can differentiate with respect to x and rearrange to obtain a decoupled pair of second-order differential equations for $x \neq 0$:

$$v_0^2 \frac{d^2 \tilde{P}_\pm(x,s)}{dx^2} - \left[(s+\gamma)^2 - \gamma^2\right] \tilde{P}_\pm(x,s) = 0. \tag{110}$$

As the boundary conditions impose that P_+ and P_- are finite as $x \to \infty$, we uncover the solutions

$$\tilde{P}_\pm = \begin{cases} A_\pm e^{-\lambda_s x}, & x > 0 \\ B_\pm e^{+\lambda_s x}, & x < 0 \end{cases} \tag{111}$$

where we define $\lambda_s = \lambda(s) = \sqrt{(s(s+2\gamma))/v_0^2}$.

We know that the total probability is symmetric about 0 due to invariance under time reversal and the symmetry of the initial condition. This implies that $A_+ + A_- = B_+ + B_-$. Furthermore, $\int_{\mathbb{R}} dx\, [\tilde{P}_+ + \tilde{P}_-] = 1/s$, we must have that $A_+ + A_- = B_+ + B_- = \frac{\lambda_s}{2s}$. Using this result, we find that the Laplace transform of the probability density, $P_0(x,t)$, of an RTP with position x at time t is

$$\tilde{P}_0(x,s) = \tilde{P}_+(x,s) + \tilde{P}_-(x,s) = \frac{\lambda_s}{2s} e^{-\lambda_s |x|}. \tag{112}$$

This can be inverted to find that

$$P_0(x,t) = \frac{e^{-\gamma t}}{2}\left\{\delta(x-v_0t)+\delta(x+v_0t)+\frac{\gamma}{v_0}\left[I_0(\alpha)+\frac{\gamma t}{\alpha}I_1(\alpha)\right]\Theta(v_0t-|x|)\right\}, \tag{113}$$

where I_0 and I_1 are modified Bessel functions of the first kind, Θ is the Heaviside function and $\alpha = \frac{\gamma}{v_0}\sqrt{v_0^2t^2-x^2}$.

4.2 Steady state under resetting

We introduce the resetting protocol where the RTP resets to $X_r = 0$ at rate r where, at each reset, the velocity is randomised to $+v_0$ or $-v_0$, each with probability 1/2. Using a similar renewal approach as in previous sections, outlined in [18], we obtain the renewal equation which expresses the probability with resetting, $P(x,t)$, in terms of the probability without resetting, $P_0(x,t)$,

$$\begin{aligned} P(x,t) &= e^{-rt}P_0(x,t) + \int_0^t d\tau r e^{-r\tau}P_0(x,\tau)\int_{\mathbb{R}} dy\, P(y,t-\tau) \\ &= e^{-rt}P_0(x,t) + \int_0^t d\tau\, r e^{-r\tau}P_0(x,\tau), \end{aligned} \tag{114}$$

where the first term corresponds to the contribution from no reset having occurred and the integral term corresponds to the contribution from resets occurring at times in the interval $[0,t]$ and at positions y. The integral over y equals 1 since it is a probability distribution.

The corresponding steady-state distribution can be derived by taking the limit as $t\to\infty$,

$$P_\infty(x) = \lim_{t\to\infty} P(x,t) = r\int_0^\infty dt\, e^{-rt}P_0(x,t) = r\tilde{P}_0(x,r) \tag{115}$$

Using equation (112), we obtain that the steady state of an RTP under resetting is

$$P_\infty(x) = \frac{\lambda_r}{2}\exp(-\lambda_r|x|) \tag{116}$$

We observe the same general behaviour as in the diffusive case, in which the NESS takes the form of a two-sided exponential (see figure 6). In fact, as we show in section 4.3, this distribution is identical to the purely diffusive result in the so-called diffusive limit.

4.3 Relationship between run-and-tumble and diffusion

We note an important time-scale of the system, $\tau_c = 1/\gamma$ [32], such that at very small times ($\tau \ll \tau_c$), the behaviour of the particle is dominated by ballistic motion and at large times ($\tau \gg \tau_c$), the particle behaves diffusively. Equivalently, we can consider the critical length-scale, $\ell_c = v_0/\gamma$ [33]. We observe that at larger lengths ($\ell \gg \ell_c$), the particle behaves more diffusively and at smaller lengths ($\ell \ll \ell_c$), the particle behaves in a more ballistic way. This difference becomes increasingly significant when we consider search processes for targets at greater distance from the initial and resetting positions.

Furthermore, an important result is that when $\gamma, v_0 \to \infty$ in the so-called *diffusive limit*, in which their ratio remains fixed as

$$\lim_{\gamma,v_0\to\infty}\frac{v_0^2}{\gamma} = 2D, \tag{117}$$

run-and-tumble motion tends to diffusion, with diffusion constant D [18]. Under the diffusive limit,

$$\lambda_r = \sqrt{(r(r+2\gamma))/v_0^2} \to \alpha_0. \tag{118}$$

Using this limit, we see that the steady-state distribution for run-and-tumble motion is the same as that of a purely diffusive particle, as in equation (17). Additionally, we observe that the NESS of the run-and-tumble model relaxes to the NESS in the diffusion model as it approaches its diffusive limit. This behaviour can be observed in figure 6. Moreover, in subsequent sections, we observe that the limiting behaviour of other characteristics, such as the MFPT and the optimal resetting rate also tend to those given by the diffusion model under the diffusive limit. These results are presented in figure 8.

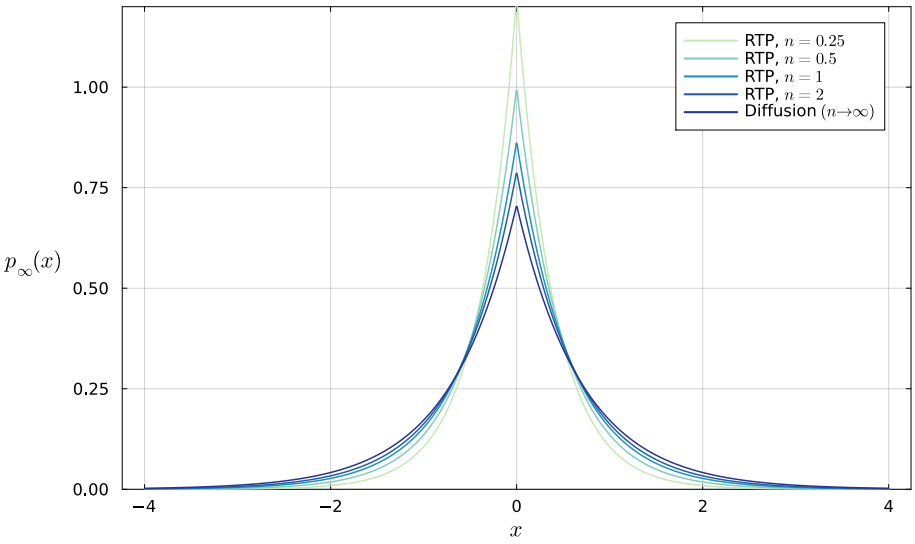

Figure 6 The steady-state distribution of an RTP under stochastic resetting, for $\gamma = n, v_0 = \sqrt{n}$ in the diffusive limit ($n \to \infty$) with $D = 1/2$. We observe that for these values, even for small n, we have a very similar steady state.

4.4 Optimal resetting in 1D

In this section, we show, as in [34], that the MFPT to a point on the real line becomes finite when resetting is introduced, akin to the result in the diffusive case.

4.4.1 Survival probability and the MFPT

We consider the case where the RTP resets with rate r to $X_r \geq 0$ with velocity randomisation as above. The absorbing target in this case will be the origin. In this subsection, we follow the same approach as in [18].

Analogous to the the last renewal equation for $P(x,t)$, given in equation (114), there exists a renewal equation for the survival probability for absorption, $Q_r(x_0,t)$, where $x_0 \geq 0$ is the initial position of the RTP,

$$Q_r(x_0,t) = e^{-rt}Q_0(x_0,t) + r\int_0^t d\tau\, e^{-r\tau}Q_0(X_r,\tau)Q_r(x_0,t-\tau). \tag{119}$$

By taking the Laplace transform of both sides, we obtain a representation for the survival

probability with resetting in terms of the survival probability without resetting

$$\begin{aligned}\tilde{Q}_r(x_0, s) &= \tilde{Q}_0(x_0, r+s) + r\tilde{Q}_0(X_r, r+s)\tilde{Q}_r(x_0, s) \\ &= \frac{\tilde{Q}_0(x_0, r+s)}{1 - r\tilde{Q}_0(X_r, r+s)}.\end{aligned} \tag{120}$$

Using this equation, it remains to find the survival probability without resetting. Once again, we make use of the backward master equations which, in the case of an RTP in one dimension without resetting, are given by [34] as

$$\frac{\partial Q_+(x,t)}{\partial t} = v_0 \frac{\partial Q_+(x,t)}{\partial x} - \gamma Q_+(x,t) + \gamma Q_-(x,t), \tag{121a}$$

$$\frac{\partial Q_-(x,t)}{\partial t} = -v_0 \frac{\partial Q_-(x,t)}{\partial x} - \gamma Q_-(x,t) + \gamma Q_+(x,t), \tag{121b}$$

where Q_+ and Q_- denote the survival probabilities of an RTP starting at x with positive and negative initial velocities respectively. Once again, we take the Laplace transforms of Q_+ and Q_-, rearrange, and impose the initial conditions $Q_-(x,0) = 1$ and $Q_+(x,0) = 1$ to obtain

$$-1 = +v_0 \frac{\partial \tilde{Q}_+(x,s)}{\partial x} - (s+\gamma)\tilde{Q}_+(x,s) + \gamma \tilde{Q}_-(x,s), \tag{122a}$$

$$-1 = -v_0 \frac{\partial \tilde{Q}_-(x,s)}{\partial x} - (s+\gamma)\tilde{Q}_-(x,s) + \gamma \tilde{Q}_+(x,s). \tag{122b}$$

Following a similar approach to section 4.1, we solve the system under the boundary condition $Q_-(0,t) = 0$ to find the following expressions for $\tilde{Q}_+$ and $\tilde{Q}_-$

$$\tilde{Q}_+(x_0, s) = \frac{1}{s} + \frac{1}{\gamma s}(v_0\lambda_s - (s+\gamma))e^{-\lambda_s x_0}, \tag{123a}$$

$$\tilde{Q}_-(x_0, s) = \frac{1}{s}(1 - e^{-\lambda_s x_0}), \tag{123b}$$

where $\lambda_s = \sqrt{s(s+2\gamma)/v_0^2}$. To find $\tilde{Q}_0$, we sum the above expressions and substitute into equation (120), in which we observe divergence at $s \to 0$, recovering the result that MFPT is infinite in the absence of resetting. Thus, we obtain an expression for $\tilde{Q}_r$ under the simplifying assumption that $x_0 = X_r$

$$\tilde{Q}_r(x_0 = X_r, s) = -\frac{1}{r} + \frac{1}{r}\left[\frac{2\gamma(s+r)\exp(\lambda_{s+r}X_r)}{2\gamma s \exp(\lambda_{s+r}X_r) - r[v_0\lambda_{s+r} - (r+s+2\gamma)]}\right]. \tag{124}$$

As discussed in section 2.3.1, we use the survival probability to recover the mean first-passage time to the origin. In this case, the MFPT, $T(X_r)$ is given by $\tilde{Q}_r(X_r, 0)$, as in equation (30)

$$T_{\mathrm{RTP}}(X_r = x_0) = -\frac{1}{r} + \frac{2\gamma}{r}\left[\frac{e^{\lambda_r X_r}}{r + 2\gamma - (r(r+2\gamma))^{1/2}}\right]. \tag{125}$$

Under the diffusive limit, using (118), we recover the result for pure diffusion, as established in equation (31).

4.4.2 Optimal parameters with reset

We observe that $T_{\mathrm{RTP}}(X_r = x_0)$ diverges as $r \to 0$ and $r \to \infty$. This implies that there exists an optimal value of r such that T_{RTP} is minimised, analogous to the diffusive case.

We wish to compare the mean first-passage times for diffusion and run-and-tumble, so we follow the approach in [18], and introduce the compound variables

$$R \equiv \frac{r}{2\gamma} \text{ and } \xi \equiv \frac{2\gamma X_r}{v_0},$$

in terms of which, we have that for $T_{\mathrm{RTP}}(X_r = x_0)$,

$$2\gamma T_{\mathrm{RTP}}(R,\xi) = -\frac{1}{R} + \frac{\exp\left((R(1+R))^{1/2}\xi\right)}{R\left[1+R-(R(1+R))^{1/2}\right]}. \tag{126}$$

To compare optimal reset rates, r, we fix $\gamma = 1/2$, $D = v_0^2/2\gamma = 1$, and $X_r = x_0 = 1$. This recovers the diffusive result in figure 3. As $R = r$, we can minimise the expression for T_{RTP} presented in equation (126) and therefore determine the optimal value of R, $r_{\mathrm{RTP}} \approx 0.55873$. Thus, we directly compare the optimal rate of reset that minimises the MFPT, which we present in figure 7.

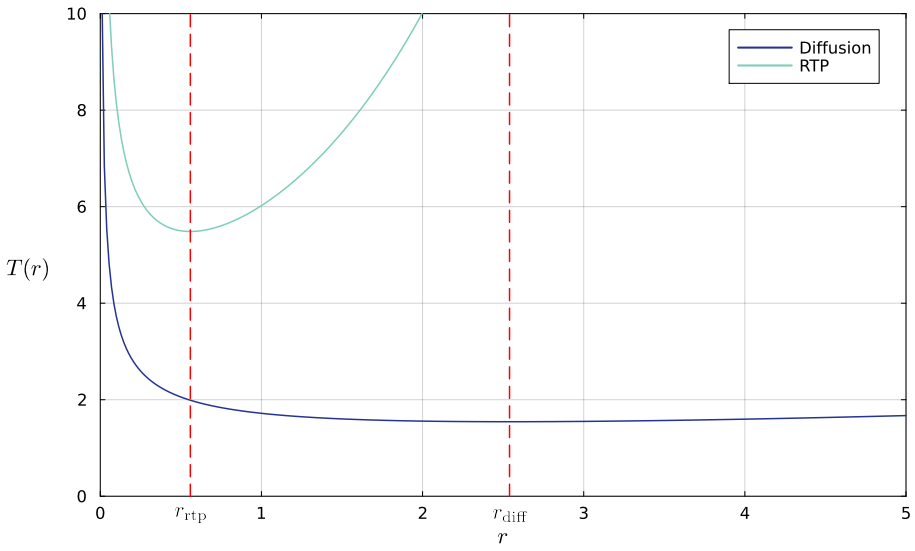

Figure 7 MFPT in the run-and-tumble and diffusion models plotted against r for $\gamma = 1/2$, $D = v_0^2/2\gamma = 1$, and $X_r = x_0 = 1$. We find that $r_{\mathrm{RTP}} \approx 0.55873$ is less than $r_{\mathrm{diff}} = r^* \approx 2.53962$, for the diffusive case. Furthermore, the optimal mean first-passage time for run-and-tumble is much larger, $T_{\mathrm{RTP}}(r_{\mathrm{RTP}}) \approx 5.48571$, than that of diffusion, $T(r_{\mathrm{diff}} = r^*) \approx 1.54414$ [18].

In the case that the particle starts sufficiently far away from the absorbing target, the mean first-passage time is longer and therefore resembles a diffusive particle. However, a particle that starts sufficiently close to the absorbing target differs from a purely diffusive and the ballistic motion dominates. As explored previously, an RTP becomes more diffusive at larger time-scales. We observe this transition in figure 8(a) and the increase of the optimal rate as the run-and-tumble becomes more diffusive in figure 8(b).

5 Run-and-tumble particles with resetting in 2D

The dynamics of an RTP extend naturally into higher dimensions. In 2D, the particle is re-oriented randomly at each tumble to an angle $\theta \in [0, 2\pi)$. Particles reset to a point X_r with

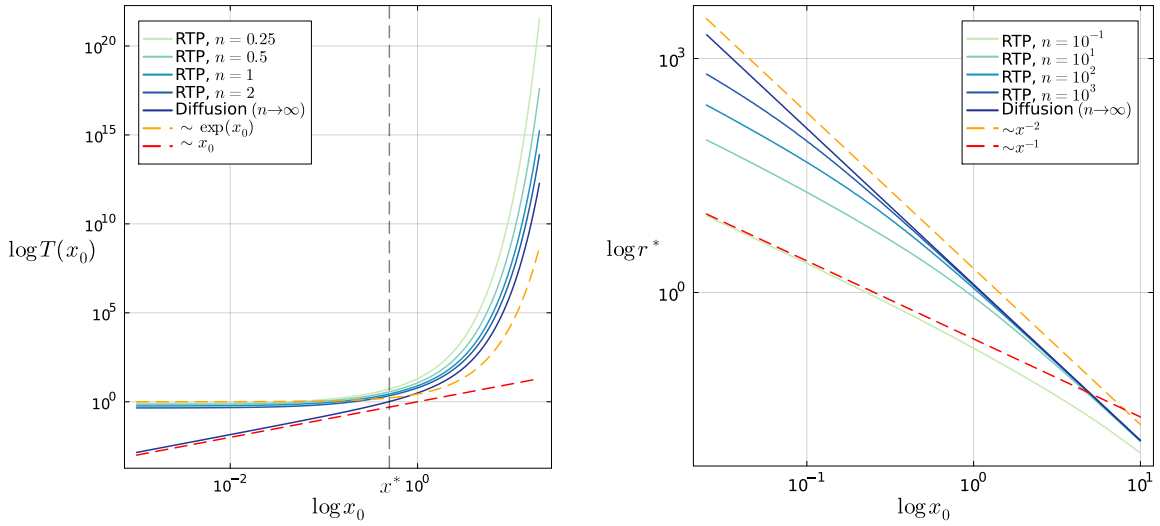

(a) Mean first-passage time.

(b) Optimal resetting rate.

Figure 8 Comparing the MFPT and the optimal resetting rate r^* as functions of x_0 for run-and-tumble particles in the diffusive limit, with $\gamma = n, v_0 = \sqrt{n}, D = 1/2$ and, in the case of figure 8(a), $r = 1$. We observe a divergence in the MFPT behaviour around $x_0 = x^* = v_0/(\gamma + r)$, which corresponds to starting at a short distance, where run-and-tumble particles cannot be modelled as diffusive.

rate r and proceed ballistically at a randomised orientation. In this section, we present the steady state under resetting and explore how certain characteristics of run-and-tumble particles compare with those explored for diffusion.

5.1 Extension to 2D: Fokker-Planck equation and NESS

The Fokker-Planck equation for an RTP which starts at the origin and initial orientation θ_0 without resetting is given in [32] to be:

$$\frac{\partial P_0(\vec{x}, \theta, t|\theta_0)}{\partial t} = -\hat{n} \cdot \nabla P_0(\vec{x}, \theta, t|\theta_0) - \gamma P_0(\vec{x}, \theta, t|\theta_0) + \frac{\gamma}{2\pi} \int d\phi P_0(\vec{x}, \phi, t|\theta_0), \tag{127}$$

where $P_0(\vec{x}, \theta, t|\theta_0)$ is the probability that the particle is at position $\vec{x}$ and orientation θ at time t given that it starts at the origin with orientation θ_0, and $\hat{n} = (\cos\theta, \sin\theta)$ is the unit vector in the direction of θ. As in [32], we present explicit forms for the marginal radial- and marginal x-distributions

$$P_0(\rho, t) = e^{-\gamma t}\left[\delta(\rho - v_0 t) + \frac{\gamma\rho}{v_0} \frac{\exp(\frac{\gamma}{v_0}\sqrt{v_0^2 t^2 - \rho^2})}{\sqrt{v_0^2 t^2 - \rho^2}} \Theta(v_0 t - \rho)\right], \tag{128}$$

$$P_0(x, t) = e^{-\gamma t}\left(\frac{1}{\pi\sqrt{v_0^2 t^2 - x^2}} + \frac{\gamma}{2v_0}\left[L_0\left(\frac{\gamma}{v_0}\sqrt{v_0^2 t^2 - x^2}\right) + I_0\left(\frac{\gamma}{v_0}\sqrt{v_0^2 t^2 - x^2}\right)\right]\right), \tag{129}$$

where I_ν is the modified Bessel function of the first kind of order ν and where L_0 is the modified Struve function.

The resetting mechanism we consider is such that the particle resets to its initial position only (i.e. $\vec{X}_r = \vec{x_0}$). Using a similar renewal approach to previous sections, we find that there

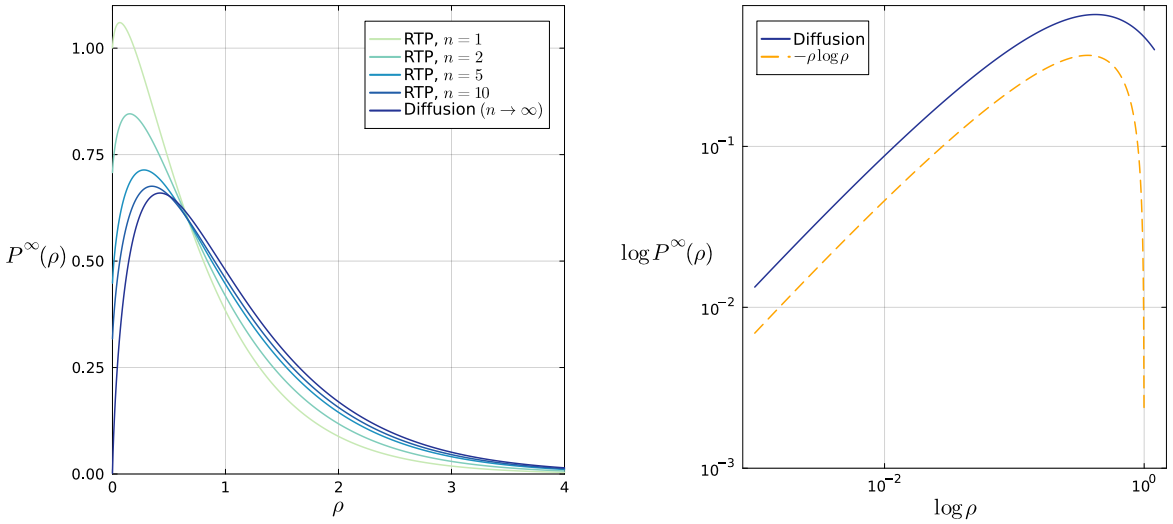

(a) Marginal radial-distribution.

(b) Decay rate for diffusive case.

Figure 9 We plot the marginal radial-distributions with parameters $\gamma = n, v_0 = \sqrt{n}, D = 1/2, r = 1$. In figure 9(a), we show how the marginal radial-distribution of the RTP attains a finite value for $\rho = 0$ whereas the marginal radial-distribution for diffusion vanishes as $\rho \to 0$. Additionally in figure 9(b), the marginal radial-distribution for diffusion goes to 0 like $\rho \log \rho$ and this is plotted.

is an NESS distribution for the marginal radial- and x-distributions, which are analogous to the results derived for diffusion under resetting.

The marginal radial- and x-steady-state distributions for $\vec{x}_0 = \vec{X}_r = 0$, P^{∞}_{rad} and P^{∞}_{x}, are given in [32] to be

$$P^{\infty}_{\text{rad}}(\rho) = \frac{r}{v_0} e^{-(r+\gamma)\frac{\rho}{v_0}} + \frac{r\gamma\rho}{v_0} \int_{\frac{\rho}{v_0}}^{\infty} \mathrm{d}s \frac{e^{-(r+\gamma)s} \exp\left(\frac{\gamma}{v_0}\sqrt{v_0^2 s^2 - \rho^2}\right)}{\sqrt{v_0^2 s^2 - \rho^2}} \tag{130}$$

$$\begin{aligned} P^{\infty}_{\text{x}}(x) = r \int_{|x|/v_0}^{\infty} \mathrm{d}s \, \frac{e^{-(\gamma+r)s}}{\pi\sqrt{v_0^2 s^2 - x^2}} \\ + \frac{r\gamma}{2v_0} \int_{|x|/v_0}^{\infty} \mathrm{d}s \, e^{-(\gamma+r)s} \left[L_0\left(\frac{\gamma}{v_0}\sqrt{v_0^2 s^2 - x^2}\right) + I_0\left(\frac{\gamma}{v_0}\sqrt{v_0^2 s^2 - x^2}\right)\right]. \end{aligned} \tag{131}$$

The marginal radial-steady-state distribution of a diffusive particle can be derived from (78) by integrating over all $\vec{x}$ such that $|\vec{x}| = \rho$. We observe that the distribution vanishes at $\rho = 0$ at a rate of $\rho \log \rho$, as shown in figure 9(b). This result implies that the purely diffusive steady state overpowers resetting at the origin when considering the marginal radial-steady-state distribution. This differs from that of a 2D RTP, which is finite at 0 [32]. We plot this in figure 9(a).

Furthermore, the marginal x-steady-state distribution of a 2D diffusive particle under resetting is given in [25], is finite at 0 and decays exponentially for $|\vec{x}| > 0$. Conversely, the marginal x-steady-state distribution of an RTP in 2D diverges logarithmically at the origin. An exponential decay is also exhibited for large $|\vec{x}|$.

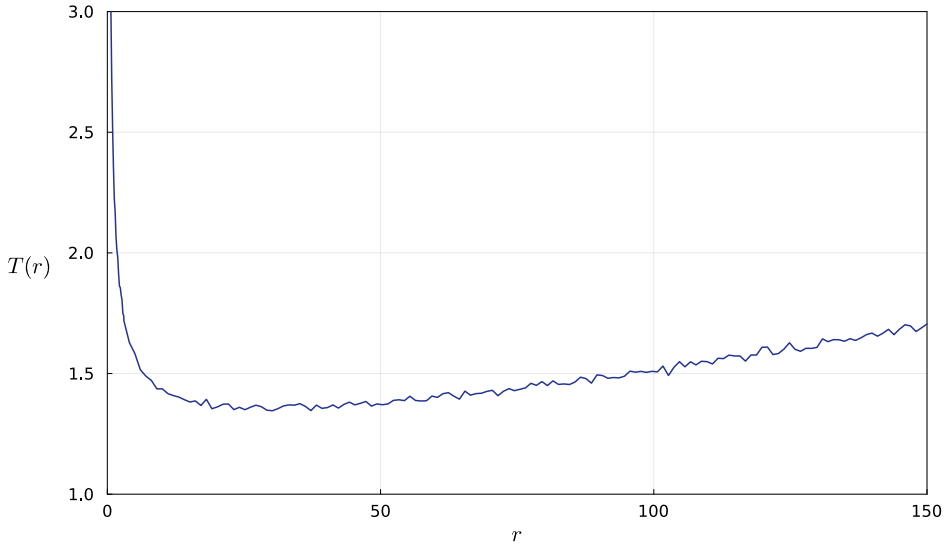

Figure 10 Numerical results plotting the mean first-passage time for an RTP in $d = 2$, with parameters $X_r = x_0 = (0.76, 0)$, $a = 0.75$, $\gamma = v_0 = 1$. We observe divergence as $r \to 0$ and $r \to \infty$, and a minimum value for MFPT.

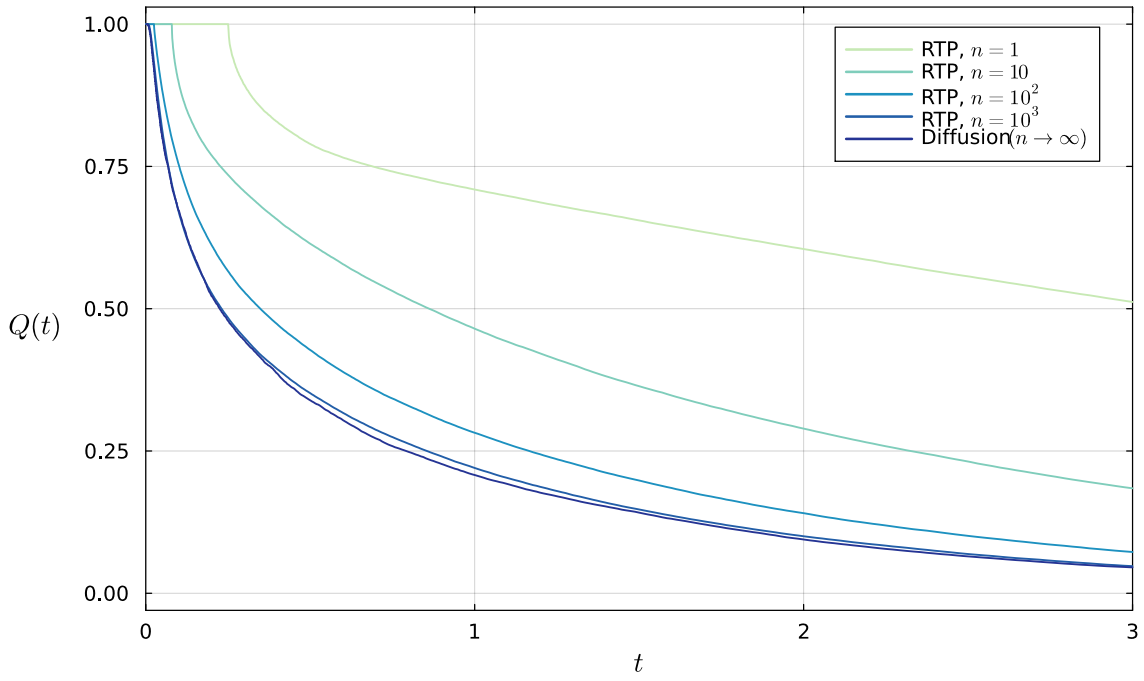

Figure 11 Survival probabilities simulated for 2D run-and-tumble and diffusive particles with $a = 0.75$, $\vec{x}_0 = (1, 0)$, $D = 1/2$, $v_0^2 = \gamma = n$. We observe that the survival probabilities for run-and-tumble particles are generally higher than the diffusive case and that these converge in the diffusive limit. Furthermore, for RTPs with small v_0, we observe there exists a minimal time before the particle can be absorbed, which is given by $\mathrm{dist}(\text{boundary of target}, x_0)/v_0$. This is reflected by the initial flat-lining.

5.2 Survival probability and MFPT to an absorbing circle at the origin

The survival probability for a run-and-tumble particle in 2D is difficult to solve analytically in general cases because the orientation of the velocity is a continuous random variable [32, 35]. While diffusion can be seen as the continuum limit of a random walk on a lattice, run-and-tumble motion cannot be considered discretely [36]. Therefore, the approach followed in section 3.3 cannot be applied to solving the backwards master equation in this case due to the continuity of the reorientation distribution. This marks a key difference from the one-dimensional case. Therefore, we employ numerical methods to elucidate the behaviour of run-and-tumble searches for various absorbing targets. As in the diffusive case, we observe that by introducing resetting the mean first-passage time is rendered finite, and an optimal resetting rate can be found in some cases.

In particular, we examine the survival probabilities and MFPT of a run-and-tumble particle starting at x_0, resetting to X_r with rate r and in the presence of an absorbing circle of radius a centred at the origin with the aim of comparing it with the derived behaviour for a diffusive particle. We can apply this to modelling the motion of a bacterium searching for food, where the absorbing circle is a food source.

We know the introduction of resetting makes the mean first-passage time finite. We show numerically that the non-monotone behaviour of the MFPT in figure 10 matches the 2D diffusive case. Additionally, we show that the survival probability for run-and-tumble (with $v_0^2/\gamma = 2D$) is initially higher than the survival probability for diffusion where we approach the diffusive limit, as presented in figure 11. This suggests that the MFPT for an RTP is higher than that of a diffusive particle with the same set of parameters, which we expect, given the behaviour observed in 1D.

Thus, we see that resetting renders the MFPT finite, and we observe an optimal constant resetting rate due to the non-monotonicity of the MFPT with respect to r. Therefore, we may optimise run-and-tumble search processes in 2D for an absorbing circle centered at the origin.

5.3 Many Poisson-distributed static traps

As explored in the diffusive case, we may also consider an RTP in a sea of static traps. Over large time-scales (corresponding to low densities of traps) we expect similar behaviour. However, over short time-scales, we expect their behaviour to differ significantly. Intuitively, if the RTP is absorbed before it has a chance to tumble, then its behaviour is purely ballistic.

We have a sea of Poisson-distributed traps in $\mathbb{R}^2$, as described in section 3.4. This is governed by a density parameter ρ. In this setting, our particles reset at constant rate $r = 1$ to a random position.

As we are considering the difference in behaviour, we define $Q_{\text{diff}}(t)$ and $Q_{\text{RTP}}(t)$, the survival probabilities for diffusive particles and RTPs respectively, and we analyse the behaviour of $Q_\Delta(t) \equiv Q_{\text{diff}}(t) - Q_{\text{RTP}}(t)$, the difference between these survival probabilities. As shown in figure 12, we observe unexpected behaviour: there is a critical density at $\rho = 1$. For $\rho > 1$, we observe faster decay in $Q_\Delta(t)$, which corresponds to the RTP process approaching diffusion faster. For $\rho < 1$, we find that the RTP process resembles diffusion less quickly, although we observe that Q_Δ exhibits exponential decay for all values of ρ.

We have previously observed (see figure 7) that run-and-tumble particles exhibit a higher MFPT than diffusive particles. We conjecture that this is due to the presence of only a single target, so it is possible for the ballistic component of an RTP to 'miss' entirely, which greatly increases the MFPT. However, at greater densities in the 2D case, it becomes impossible for the

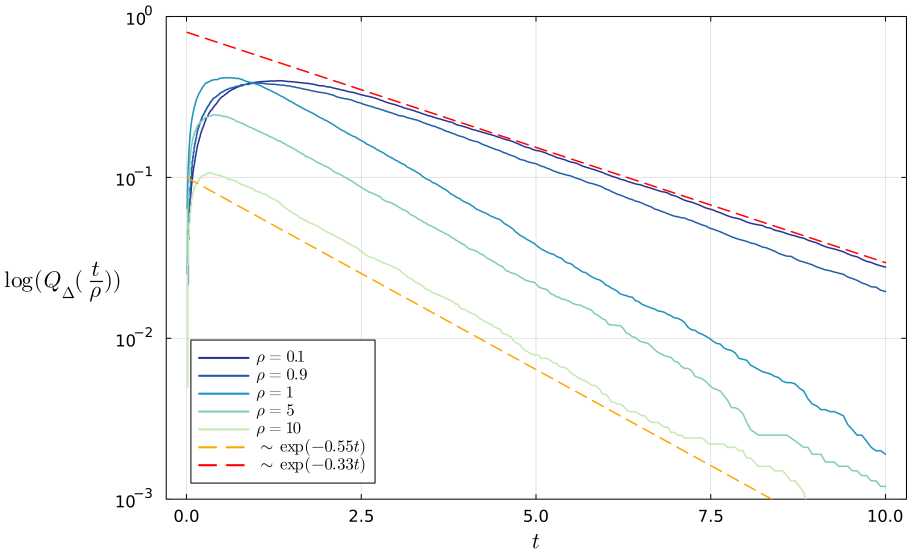

Figure 12 Numerically, we observe unexpected behaviour. There is a critical point for $\rho = 1$; greater density results in the process becoming diffusive much faster. We attribute this to ballistic particles being absorbed much faster, leading to Q_Δ becoming dominated by only particles which have undergone many tumbles, i.e. are more diffusive. We plot for t/ρ to more easily compare the curves; Q_Δ decays $\sim \exp(-\lambda\rho t)$ for some λ.

RTP to 'miss'. Therefore, the RTPs that do not tumble (i.e. behave ballistically) are absorbed more quickly. Thus, Q_Δ is dominated by the RTPs that have tumbled many times, i.e. the most diffusive particles.

We now provide an interpretation of our critical point $\rho = 1$. We consider the 1D problem in which a particle starts at $x = 0$, between two absorbing boundaries at $x = \pm L$. It is known that the MFPT for a particle under diffusion is $\tau_{\text{diff}} = L^2/2D \equiv \gamma L^2/v_0^2$ [37], and for an RTP the MFPT is $\tau_{\text{rtp}} = L/v_0 + \gamma L^2/2v_0^2$ [38]. Upon making the substitution $\gamma = v_0 = 1$, we observe that $\tau_{\text{diff}} = L^2, \tau_{\text{rtp}} = L + L^2/2$, and we note that for $L < 2, \tau_{\text{diff}} < \tau_{\text{rtp}}$, and for $L > 2, \tau_{\text{diff}} > \tau_{\text{rtp}}$. It can be shown that for static Poisson-distributed traps with radius a, the mean free path before encountering a trap is given by $1/2a\rho$, and for $a = 1/4, \rho = 1$, we obtain a mean free path of 2: the value for which τ_{diff} eclipses τ_{rtp}.

6 Conclusion

In this paper, we have summarised many of the key results in stochastic resetting, and how it pertains to two primary cases - a diffusive particle and a run-and-tumble particle. In particular, we have shown that the MFPT can be optimised with a certain resetting rate r, and we have explored different resetting schemes, including: resetting to a distribution, time-dependent resetting, and space-dependent resetting. We have looked at common extensions to this problem, notably the presence of drift/potentials and higher dimensions, and briefly discussed the chemical applications of the model. For run-and-tumble particles, we explore similar results, and compare them with those for diffusion, recovering the latter results in the diffusive limit.

We also provided numerical results, both to supplement analytic results and to explore the short- and long-term behaviours of diffusive and run-and-tumble particles in a sea of static traps.

We note that in the presence of resetting to a random location, exponential decay of survival probability is recovered due to the probability of resetting onto a trap. Furthermore, periodic point patterns do not fall under assertions about slow decay, and appear to exhibit exponential decay numerically.

Finally, we have considered the impact of density of Poisson-distributed traps on the first passage properties. Crucially we found that there exists a critical density below which the ballistic nature of the run and tumble particle dominates and dictates the first passage properties.

Possible future avenues of research include whether analytic results can be found in higher dimensions beyond asymptotic behaviour, and the evolution of the system under more complex trapping setups. The change in asymptotic behaviours motivates a question of how stochastic resetting changes the long-term behaviours of other systems, particularly when behaviour is dominated by a few rare initial configurations of some random state (such as a large trap-free region in 3.4).

We also note that in order to experimentally verify these predictions, we often are required to devise specific resetting processes which may differ from simplistic models. We formulate one such example in this paper (resetting to a normal distribution) and mention several others briefly in the introduction. New experimental procedures could give rise to new resetting paradigms that would require further study.

Acknowledgments

We wish to thank Dr. Thibault Bertrand for his support and guidance as our supervisor.

A Appendix A: Solving for MFPT

We seek to obtain a solution to

$$-1 = D\frac{\partial^2 T(x)}{\partial x^2} - rT(x) + rT(x_0). \tag{132}$$

Letting $\alpha_0 = \sqrt{r/D}$, the general solution to equation (132) has the form [12]

$$T(x) = Ae^{\alpha_0 x} + Be^{-\alpha_0 x} + \frac{1 + rT(x_0)}{r}. \tag{133}$$

Since $T(x)$ is finite as $x \to \infty$, we have $A = 0$. Applying our second boundary condition,

$$T(0) = B + \frac{1 + rT(x_0)}{r} = 0 \implies B = -\frac{1 + rT(x_0)}{r}. \tag{134}$$

Thus, we obtain the solution presented in equation (32).

B Appendix B: Numerical simulation

For our simulation, we model the position x of each particle, and update each particle at a fixed timestep dt up to some maximum time T. A diffusive particle is governed by the rule

$$\begin{aligned} x(t+dt) &= X_r \quad \text{if resetting} \\ &= x(t) + \xi(t)(dt)^{1/2} \quad \text{else,} \end{aligned} \tag{135}$$

where ξ_t is a sample drawn from a normal distribution $N(0, 2D)$, where D is the particle's diffusion coefficient. At the beginning of the simulation, each particle has a reset time τ drawn from an exponential distribution with rate parameter r. If $t + dt > \tau$, then the particle is reset.

In the 2D case, we analogously have

$$\begin{aligned} \vec{x}(t+dt) &= \vec{X}_r \quad \text{if resetting} \\ &= \vec{x}(t) + \begin{pmatrix} \xi_1(t) \\ \xi_2(t) \end{pmatrix} (dt)^{1/2} \quad \text{else,} \end{aligned} \tag{136}$$

where both ξ_1, ξ_2 are distributed as ξ in the 1D case, i.e. both coordinates of the particle undergo diffusion.

A 1D RTP is governed by the rule

$$\begin{aligned} x(t+dt) &= X_r \quad \text{if resetting} \\ &= x(t) + v_0 \sigma dt \quad \text{else,} \end{aligned} \tag{137}$$

where $\sigma \in \{1, -1\}$ is the particle's orientation, which is reversed when the particle tumbles. These tumbles are governed similarly to the resets - a tumbling time τ_γ is drawn from an exponential distribution with rate γ, and if $t + dt > \tau_\gamma$ then the particle's orientation is reversed.

For survival simulations, a particle would diffuse (or move via run-and-tumble motion) until absorbed.

In the simulations for 3.4 and 5.3, a large length l was chosen, and a $l \times l$ square centred on the origin was uniformly populated with a number of traps $N \sim \text{Exp}(\rho l^2)$. Particles 'resetting' to a random location corresponds to a resetting distribution uniform on an $l/2 \times l/2$ square about the origin. We choose l to be large compared to the diffusive particle's path such that it is extremely unlikely for the particle to leave the box.

C Appendix C: Marginal radial-steady-state distribution for a diffusive particle in 2D

Using (78) we perform the integral with $\vec{x}_0 = 0$ to obtain

$$p_\infty^{rad}(\rho) = \int_{|\vec{x}|=\rho} \frac{\alpha_0^2}{2\pi} K_0(\alpha_0|\vec{x} - \vec{x}_0|) d\vec{x} = \rho\alpha_0^2 K_0(\alpha_0|\rho|). \tag{138}$$

From the small argument behaviour of K_0, $K_0(x) \approx -\log(x/2) - \gamma_E$, we observe that $p_\infty^{rad}(\rho) \to 0$ as $\rho \to 0$.

References

[1] B. Evans and W. O'Brien. An analysis of the feeding rate of white crappie. *Developments in Environmental Biology of Fishes*, 7:299–306, Jan. 1986.

[2] E. Elbeltagi, T. Hegazy, and D. Grierson. Comparison among five evolutionary-based optimization algorithms. *Advanced Engineering Informatics*, 19(1):43–53, 2005.

[3] O. Bénichou, M. Moreau, P.-H. Suet, and R. Voituriez. Intermittent search process and teleportation. *The Journal of Chemical Physics*, 126(23):234109, 06 2007.

[4] M. R. Evans, S. N. Majumdar, and G. Schehr. Stochastic resetting and applications. *Journal of Physics A: Mathematical AND Theoretical*, 53(19), May 15 2020.

[5] S. Condamin, O. Bénichou, and M. M. Random walks and brownian motion: a method of computation for first-passage times and related quantities in confined geometries. *Phys. Rev. E*, 75, Feb. 2007.

[6] O. Bénichou, C. Loverdo, M. Moreau, and R. Voituriez. Intermittent search strategies. *Rev. Mod. Phys.*, 83:81–129, Mar 2011.

[7] M. A. Lomholt, K. Tal, R. Metzler, and K. Joseph. Lévy strategies in intermittent search processes are advantageous. *Proceedings of the National Academy of Sciences*, 105(32): 11055–11059, 2008.

[8] M. R. Evans and S. N. Majumdar. Diffusion with stochastic resetting. *Phys. Rev. Lett.*, 106: 160601, Apr. 2011.

[9] P. C. Bressloff. Search processes with stochastic resetting and multiple targets. *Phys. Rev. E*, 102:022115, Aug. 2020.

[10] G. R. Calvert and M. R. Evans. Searching for clusters of targets under stochastic resetting. *The European Physical Journal B*, 94(11):228, 2021.

[11] A. Pal, A. Kundu, and M. R. Evans. Diffusion under time-dependent resetting. *Journal of Physics A: Mathematical and Theoretical*, 49(22):225001, Apr. 2016.

[12] M. R. Evans and S. N. Majumdar. Diffusion with optimal resetting. *Journal of Physics A: Mathematical and Theoretical*, 44(43), Oct. 2011.

[13] M. Bramson and J. L. Lebowitz. Asymptotic behavior of densities in diffusion-dominated annihilation reactions. *Phys. Rev. Lett.*, 61:2397–2400, Nov. 1988.

[14] P. Grassberger and I. Procaccia. The long time properties of diffusion in a medium with static traps. *The Journal of Chemical Physics*, 77(12):6281–6284, Dec. 1982.

[15] R. A. Blythe and A. J. Bray. Survival probability of a diffusing particle in the presence of poisson-distributed mobile traps. *Physical Review E*, 67(4), 2003.

[16] A. E. Lindsay, J. C. Tzou, and T. Kolokolnikov. Optimization of first passage times by multiple cooperating mobile traps. *Multiscale Modeling & Simulation*, 15(2):920–947, 2017.

[17] H. C. Berg. *Random walks in biology*. Princeton University Press, Princeton, N.J, expanded ed. edition, 1993.

[18] M. R. Evans and S. N. Majumdar. Run and tumble particle under resetting: a renewal approach. *Journal of Physics A: Mathematical and Theoretical*, 51(47):475003, Oct. 2018.

[19] J. Mathews and R. L. Walker. *Mathematical Methods of Physics*. W. A. Benjamin, Michigan, USA, second edition, 1970.

[20] I. S. Gradshteyn and I. M. Ryzhik. *Table of Integrals, Series and Products*. Elsevier Academic Press, London, UK, seventh edition, 2007.

[21] W. Mangthas and N. W. A short-time drift propagator approach to the fokker-planck equation. *Korean Physical Society*, 84, Nov. 2023.

[22] S. Ray, D. Mondal, and S. Reuveni. Péclet number governs transition to acceleratory restart in drift-diffusion. *Phys. A: Math. Theor.*, 52:255002, May 2019.

[23] B. Besga, A. Bovon, A. Petrosyan, S. N. Majumdar, and S. Ciliberto. Optimal mean first-passage time for a brownian searcher subjected to resetting: Experimental and theoretical results. *Phys. Rev. Res.*, 2:032029, Jul. 2020.

[24] F. Faisant, B. Besga, A. Petrosyan, S. Ciliberto, and S. N. Majumdar. Optimal mean first-passage time of a brownian searcher with resetting in one and two dimensions: experiments, theory and numerical tests. *Journal of Statistical Mechanics: Theory and Experiment*, 2021(11):113203, Nov. 2021.

[25] M. R. Evans and S. N. Majumdar. Diffusion with resetting in arbitrary spatial dimension. *Journal of Physics A: Mathematical and Theoretical*, 47(28):285001, Jun. 2014.

[26] S. Redner. *A Guide to First-Passage Processes*. Cambridge University Press, 2001.

[27] M. Abramowitz and I. A. Stegun. *Handbook of mathematical functions*. United States Department of Commerce, Washington D.C., tenth edition, 1972.

[28] H. Risken. *Fokker-Planck Equation*, pages 63–95. Springer Berlin Heidelberg, Berlin, Heidelberg, 1996.

[29] M. D. Donsker and S. R. S. Varadhan. Asymptotics for the wiener sausage. *Communications on Pure and Applied Mathematics*, 28(4):525–565, 1975.

[30] G. T. Barkema, P. Biswas, and H. van Beijeren. Diffusion with random distribution of static traps. *Phys. Rev. Lett.*, 87:170601, Oct. 2001.

[31] S. Torquato and F. H. Stillinger. Local density fluctuations, hyperuniformity, and order metrics. *Physical Review E*, 68(4), Oct. 2003.

[32] I. Santra, U. Basu, and S. Sabhapandit. Run-and-tumble particles in two dimensions under stochastic resetting conditions. *Journal of Statistical Mechanics: Theory and Experiment*, 2020(11):113206, Nov. 2020.

[33] M. E. Cates and J. Tailleur. When are active brownian particles and run-and-tumble particles equivalent? consequences for motility-induced phase separation. *Europhysics Letters*, 101:20010, Feb. 2013.

[34] K. Malakar, V. Jemseena, A. Kundu, K. V. Kumar, S. Sabhapandit, S. N. Majumdar, S. Redner, and A. Dhar. Steady state, relaxation and first-passage properties of a run-and-tumble particle in one-dimension. *Journal of Statistical Mechanics: Theory and Experiment*, 2018 (4):043215, Apr. 2018.

[35] F. Mori, P. Le Doussal, S. N. Majumdar, and G. Schehr. Universal survival probability for a d-dimensional run-and-tumble particle. *Physical Review Letters*, 124(9), Mar. 2020.

[36] J.-F. Rupprecht, O. Bénichou, and R. Voituriez. Optimal search strategies of run-and-tumble walks. *Phys. Rev. E*, 94:012117, Jul. 2016.

[37] Z. Farkas and T. Fülöp. One-dimensional drift-diffusion between two absorbing boundaries: application to granular segregation. *Journal of Physics A: Mathematical and General*, 34(15):3191, apr 2001.

[38] L. Angelani. One-dimensional run-and-tumble motions with generic boundary conditions. *Journal of Physics A: Mathematical and Theoretical*, 56(45):455003, oct 2023.